Best Available
Copy
for all Pictures

AD/A-002 462

INVESTIGATION OF ULTRAVIOLET PHOTO-IONIZATION SUSTAINED DISCHARGE FOR GAS LASERS

R. C. Lind

Hughes Research Laboratories

Prepared for:

Office of Naval Research
Advanced Research Projects Agency

August 1974

003108

9

INVESTIGATION OF ULTRAVIOLET PHOTOIONIZATION SUSTAINED DISCHARGE FOR GAS LASERS

AD A 002462

R. C. LIND

AUGUST 1974

SEMIANNUAL TECHNICAL REPORT

1 JANUARY 1974 THROUGH 30 JUNE 1974

CONTRACT N00014-73-C-0287

Sponsored by
ADVANCED RESEARCH PROJECTS AGENCY
ARPA ORDER NO. 1807

Semiannual Technical Report
Contract N00014-73-C-0287
Reporting Period: 1 January 1974 through 30 June 1974

ARPA Order No. 1807
Program Code No. 3E90

Effective Date of Contract: 2 January 1973
Contract Expiration Date: 30 June 1974

Amount of Contract: $296,178.00
Principal Investigator: R.C. Lind
(213)456-6411

Scientific Officer: Director, Physics Programs
Physical Sciences Division
Office of Naval Research
Department of the Navy
800 North Quincy Street
Arlington, VA 22217

This research was supported by the Advanced Research Projects Agency of the Department of Defense and was monitored by ONR under Contract N00014-73-C-0287.

UNCLASSIFIED

SECURITY CLASSIFICATION OF THIS PAGE (When Data Entered)

REPORT DOCUMENTATION PAGE		READ INSTRUCTIONS BEFORE COMPLETING FORM
1. REPORT NUMBER N00014-73-C-0287	2. GOVT ACCESSION NO.	3. RECIPIENT'S CATALOG NUMBER
4. TITLE (and Subtitle) Investigation of Ultraviolet Photoionization Sustained Discharge for Gas Lasers		5. TYPE OF REPORT & PERIOD COVERED Semiannual Technical Rpt. 1 January 1974-30 June 1974 6. PERFORMING ORG. REPORT NUMBER
7. AUTHOR(s) R.C. Lind		8. CONTRACT OR GRANT NUMBER(s) N00014-73-C-0287
9. PERFORMING ORGANIZATION NAME AND ADDRESS Hughes Research Laboratories 3011 Malibu Canyon Road Malibu, CA 90265		10. PROGRAM ELEMENT, PROJECT, TASK AREA & WORK UNIT NUMBERS ARPA Order No. 1807 Program Code No. 3E90
11. CONTROLLING OFFICE NAME AND ADDRESS Advanced Research Projects Agency 1400 Wilson Boulevard Arlington, VA 22209		12. REPORT DATE August 1974 13. NUMBER OF PAGES 57
14. MONITORING AGENCY NAME & ADDRESS (if different from Controlling Office) Office of Naval Research Department of the Navy Arlington, VA 22217		15. SECURITY CLASS. (of this report) Unclassified 15a. DECLASSIFICATION DOWNGRADING SCHEDULE

16. DISTRIBUTION STATEMENT (of this Report)

17. DISTRIBUTION STATEMENT (of the abstract entered in Block 20, if different from Report)

18. SUPPLEMENTARY NOTES

19. KEY WORDS (Continue on reverse side if necessary and identify by block number)

Laser, Discharge, Ultraviolet Radiation, Photoionization

20. ABSTRACT (Continue on reverse side if necessary and identify by block number)

The objectives of this program are to investigate and improve ultraviolet (uv) photoionization plasma conditioning techniques, to perform the demonstration of a uv sustained electrical discharge atmospheric pressure CO_2 laser, and to establish scability limits.

Initially, fundamental experiments employing small scale (1 x 2 x 15 cm^3) discharge volumes established that in excess of 200 J/l-atm could

DD FORM 1 JAN 73 1473 EDITION OF 1 NOV 65 IS OBSOLETE

UNCLASSIFIED

SECURITY CLASSIFICATION OF THIS PAGE (When Data Entered)

be input to 1 atm CO_2 laser mixture by the uv photoionization of an added low ionization potential organic molecule. These and additional experiments led to conjectures for mixture mean free paths for certain critical CO_2, N_2, He tri-n-propylamine mixture ratios on the order of 8 cm.

Power extraction and small signal gain measurements were undertaken next using a device with a larger discharge volume (2.5 x 15 x 50 cm^3) and an improved uv source configuration. Output energies in excess of 45 J/l-atm with pulse lengths to 37 μs have been achieved.

The limits of scalability of the uv sustained plasma conditioning technique are now being addressed. A large volume (20 x 20 x 100 cm^3) discharge device has been constructed with initial testing under way. With a reduced active volume, 115 joules have been extracted from the device in initial measurements which corresponds to an energy density of 27 J/l-atm. Extensive testing of the medium and extraction properties will be undertaken during the coming period.

TABLE OF CONTENTS

LIST OF ILLUSTRATIONS

Preceding page blank

FIGURE		PAGE

ABSTRACT

The objectives of this program are to investigate and improve ultraviolet (uv) photoionization plasma conditioning techniques, to perform the demonstration of a uv sustained electrical discharge atmospheric pressure CO_2 laser, and to establish scalability limits.

Initially, fundamental experiments employing small scale ($1 \times 2 \times 15$ cm^3) discharge volumes established that in excess of 200 J/l-atm could be input to 1 atm CO_2 laser mixture by the uv photoionization of an added low ionization potential organic molecule. These and additional experiments led to conjectures for mixture mean free paths for certain critical CO_2, N_2, He tri-n-propylamine mixture ratios on the order of 8 cm.

Power extraction and small signal gain measurements were undertaken next using a device with a larger discharge volume ($2.5 \times 15 \times 50$ cm^3) and an improved uv source configuration. Output energies in excess of 45 J/l-atm with pulse lengths to 37 μs have been achieved.

The limits of scalability of the uv sustained plasma conditioning technique are now being addressed. A large volume ($20 \times 20 \times 100$ cm^3) discharge device has been constructed with initial testing under way. With a reduced active volume, 115 J have been extracted from the device in initial measurements which corresponds to an energy density of 27 J/l-atm. Extensive testing of the medium and extraction properties will be undertaken during the coming period.

I. INTRODUCTION

The objective of this program is to investigate and improve ultraviolet (uv) photoionization plasma conditioning techniques. Within the scope of this objective is the specific goal of the demonstration of a uv sustained electrical discharge atmospheric pressure CO_2 laser. The dynamics of the plasma generation in this mode are similar to those of the electron beam controlled discharge; the voltage applied to the main discharge electrodes can be reduced below that required for a self-sustained avalanche mode. The principal advantage realized in this approach is complete control of the main discharge by the uv source at all times during operation.

The attractive feature of uv sustained as opposed to e-beam sustained operation is the simplicity of construction. Specifically, a foil is not required and the high voltages needed to give efficient electron penetration of the foil are not necessary.

The crucial questions that need to be answered through the research conducted during this program are (1) whether an electron density sufficient to sustain the discharge in a CO_2 laser mixture can be produced by a uv photoionization technique; specifically, plasma densities of 10^{12} electrons/cm^3 over pulse lengths of 20 μs or longer must be attained, and (2) what the scalability parameters are for such a technique.

The first year program pursued to investigate these questions consisted basically of the following three tasks:

1. Determination of the emission spectrum and power saturation characteristics of uv spark souces operated in CO_2 laser mixture, metal vapors, and other gas additives.

2. Development of seeding techniques which will improve the photoionization efficiency of the laser medium.

3. Evaluation of uv photoionization sustained CO_2 laser gas discharge characteristics and laser performance via small signal gain and laser power output measurements.

During the first reporting period[1] results were obtained which emanated from the direction indicated by tasks one and two. The principal results (discussed in Section II) were: plasma densities required ($n_e \simeq 10^{12}$ electrons/cm^3 for >20 μs) have been demonstrated, emission spectra of spark discharges have been obtained, and a mixture mean-free path of 8 cm is conjectured for an appropriate mixture of CO_2, N_2, He and seed gas. Based on these results, baseline operating conditions for laser gas mixtures, seed gas concentrations, and uv intensities were established. These were then used as a guideline for laser measurements (Task 3) reported on during the second reporting period.[2] The principal results obtained during the second reporting period were the demonstration of up to 50 J/l-atm laser output energy in a 37 μs (total) pulse length in a 2.5 x 15 x 50 cm^3 device in a completely uv sustained mode of operation and the design of a large volume 20 x 20 x 100 cm^3 discharge device for scalability studies.

With the successful demonstration of extraction energies of 50 J/l-atm in a long pulse the objective of the next phase of the program is directed toward an understanding, through demonstration, of the scalability limits of the uv sustained scheme. This is to be accomplished by the testing of the large scale (20 x 20 x 100 cm^3) discharge device.

During the present reporting period design and construction on the large scale device have been completed. Initial measurements of input and laser extraction energy have been undertaken. To date an extraction energy of 115 J has been obtained in a configuration for which the electrode gap spacing has been adjusted to 6 cm. Based on the measured mode volume, this represents an extraction energy density of 27 J/l-atm. This preliminary result forms the basis for extensive medium testing and power extraction measurements to be made during the coming period.

II. SUMMARY OF PREVIOUS RESULTS

During the first year of the program extensive measurements had been undertaken on two crucial phases of the uv sustained plasma conditioning scheme. The first was a parametric investigation to determine achievable levels of discharge input energy. Second, as a direct result of the demonstration of the capability to obtain input discharge energy densities that would efficiently excite CO_2 laser mixtures, small signal gain distribution and power extraction measurements were performed. The results of these tests will be discussed below.

A. Input Energy and Mean Free Path Determination

The input energy measurements were performed on a small device which employed uv arc discharges located adjacent to the main discharge electrodes (see Fig. 1). Both the uv source and main discharge electrodes were mounted in a high vacuum glass enclosure to permit accurate control of the discharge environment. All internal supporting components were selected from those materials with low vapor pressure and outgassing properties and with high resistance to seed gas additives. Various mixture ratios of CO_2, N_2, He, seed gas concentrations, total pressures, and uv spark energies were studied to allow a complete mapping of obtainable sustainer energy densities.

Before presenting the results of these experiments, and in order to provide a theoretical basis for the assessment of these data, we will first discuss a calculation of the uv produced electron number density expected for such a system. In Fig. 2, the computed sustainer energy densities as a function of uv current are summarized for a wide range of gas mixtures. This calculation assumes single-step photoionization of the added seed gas (in this example, tri-n-propylamine is used) and a recombination limited plasma.

Preceding page blank

2768-1

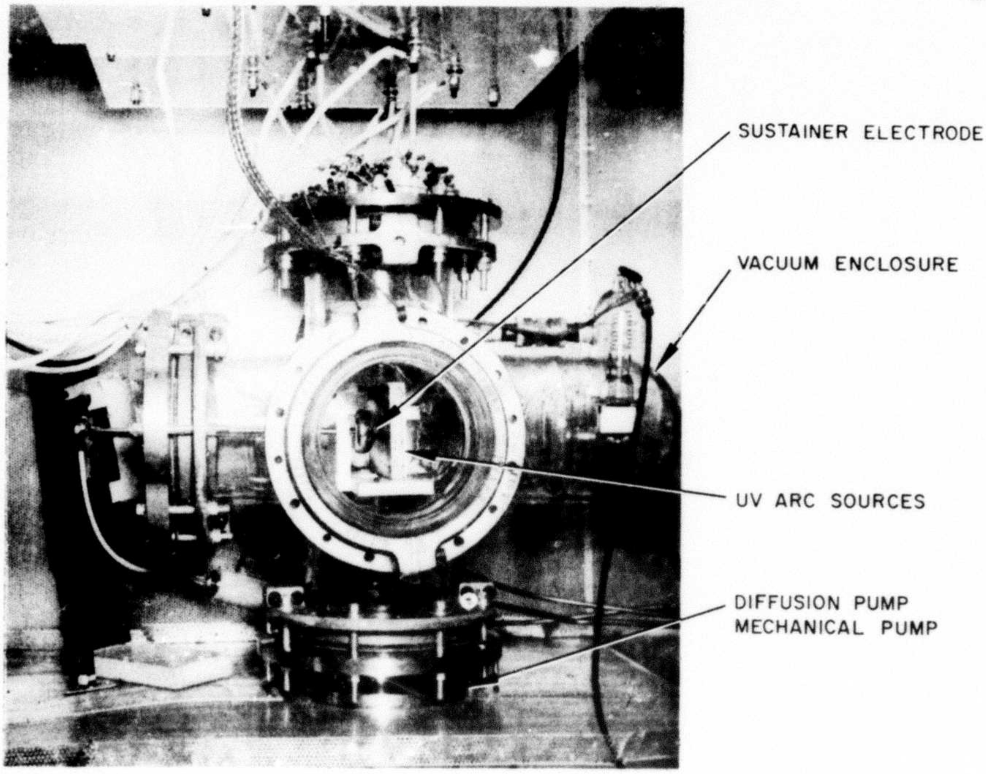

2768-2

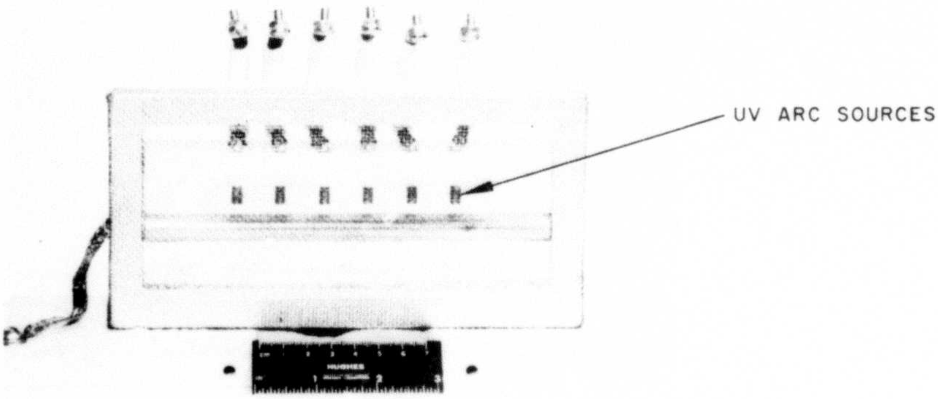

Fig. 1. Experimental uv sustained discharge device.

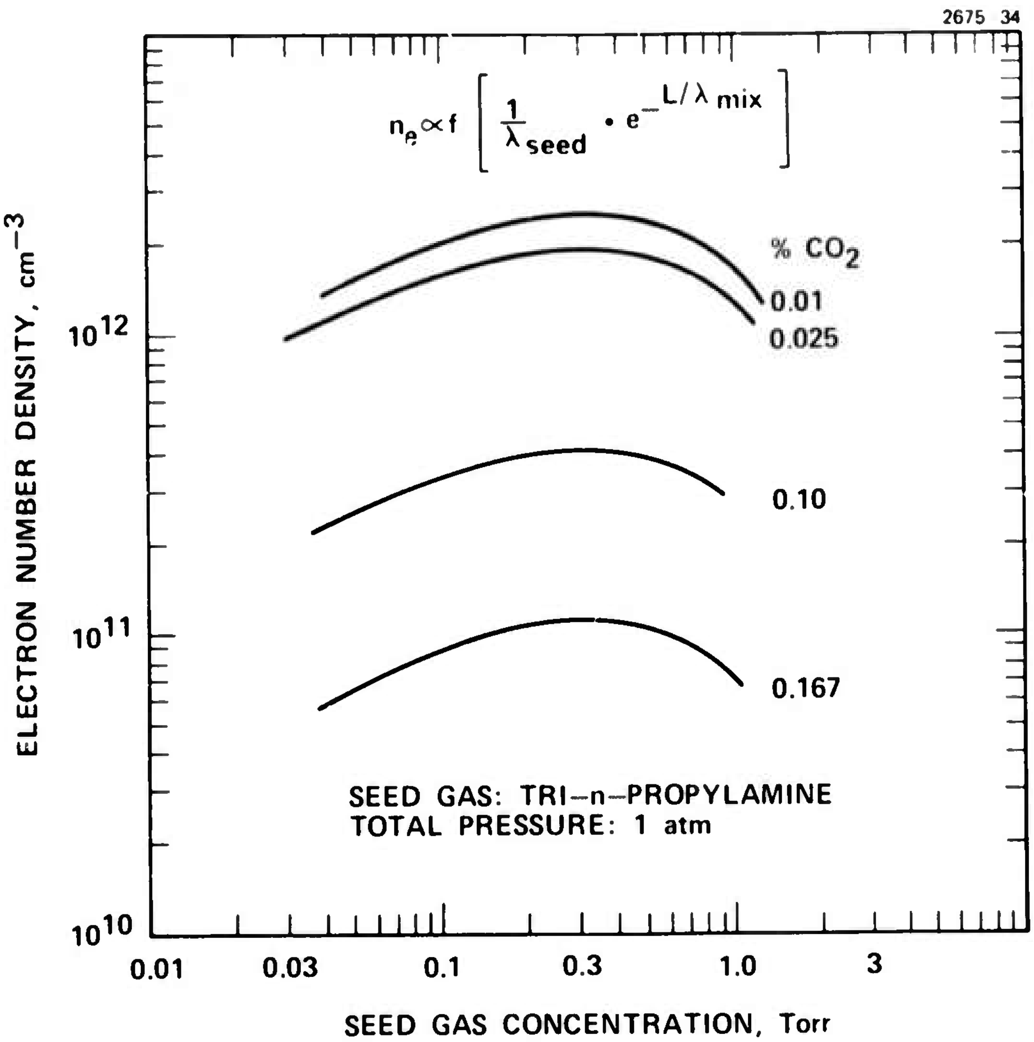

Fig. 2. Calculated electron number density.

From this figure, we see two important effects. First, there is a minimum CO_2 concentration below which no further increase in sustainer energy results. As the CO_2 concentration decreases, the effective mixture mean free path is determined by the seed gas concentration. Second, there is a broad optimum in sustainer energy for a large (order of magnitude) change in seed gas concentration which produces only a small variation in the sustainer energy, because at low seed gas concentrations the uv absorption characteristic is dictated by CO_2 molecules, and only when the seed gas concentration is increased does the seed gas absorption play a dominant role. Both of these effects are critical to the determination of the limiting mean free path and, hence, the limit of scalability.

Two results of the experimental study are shown in Figs. 3(a) and 3(b). First, in Fig. 3(a), the normalized sustainer energy obtained as a function of the normalized uv spark current is plotted for four mixture ratios and fixed seed gas concentrations while in Fig. 3(b), similar plots are for three seed gas concentrations with a fixed mixture ratio. We see that the results of these experiments follow the trends predicted above.

Figure 4 gives the absolute sustainer energies obtained for the mixture producing the largest relative energy density results shown in the previous figures. With a uv spark current of 3 kA a value of 300 J/l-atm has been obtained. The pulse lengths corresponding to these energies depend solely on the pulse length of the uv source; for the present case, this corresponds to an underdamped ringing arc circuit of approximately 50 μs in duration. Although 300 J/l-atm is the input energy requirement for efficient CO_2 excitation, a considerable amount of radiated energy is expended to achieve this level. Estimates of this energy based on the 3 kA spark current indicate that approximately equal amounts of energy are

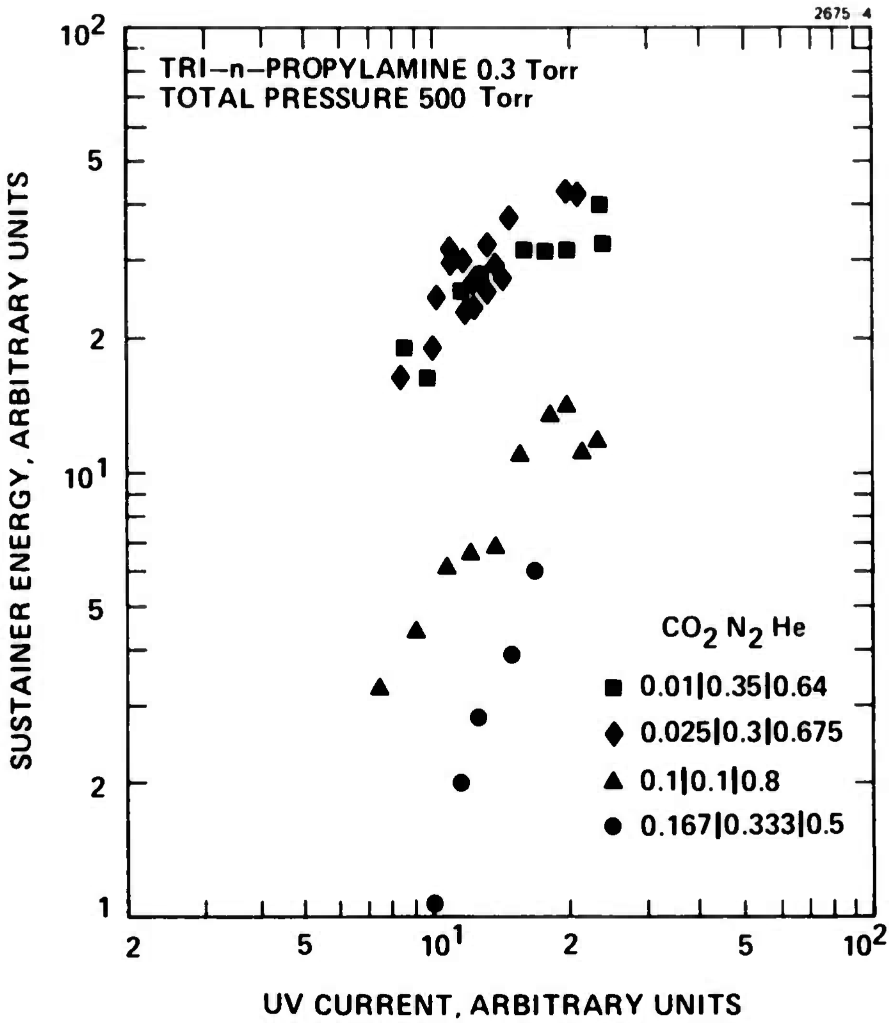

(a) For various laser mixtures.

Fig. 3. Sustainer energy as a function of uv current.

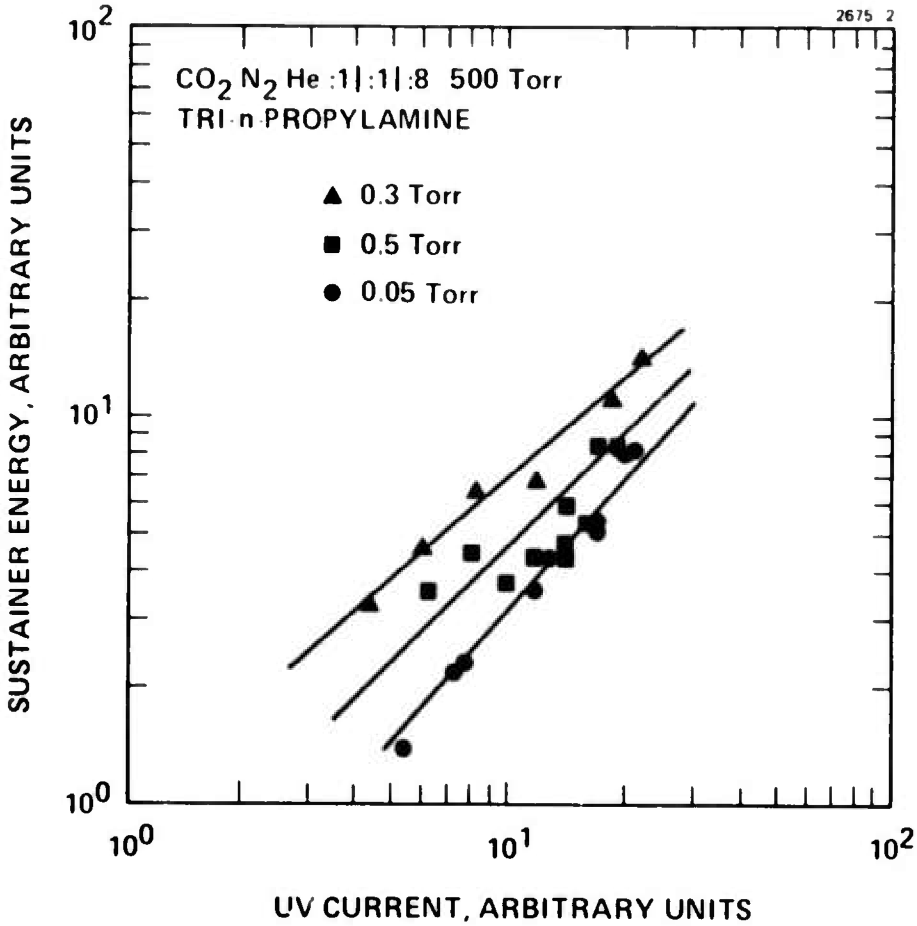

(b) For various concentrations of tri-n-propylamine.

Fig. 3. Sustainer energy as a function of uv current.

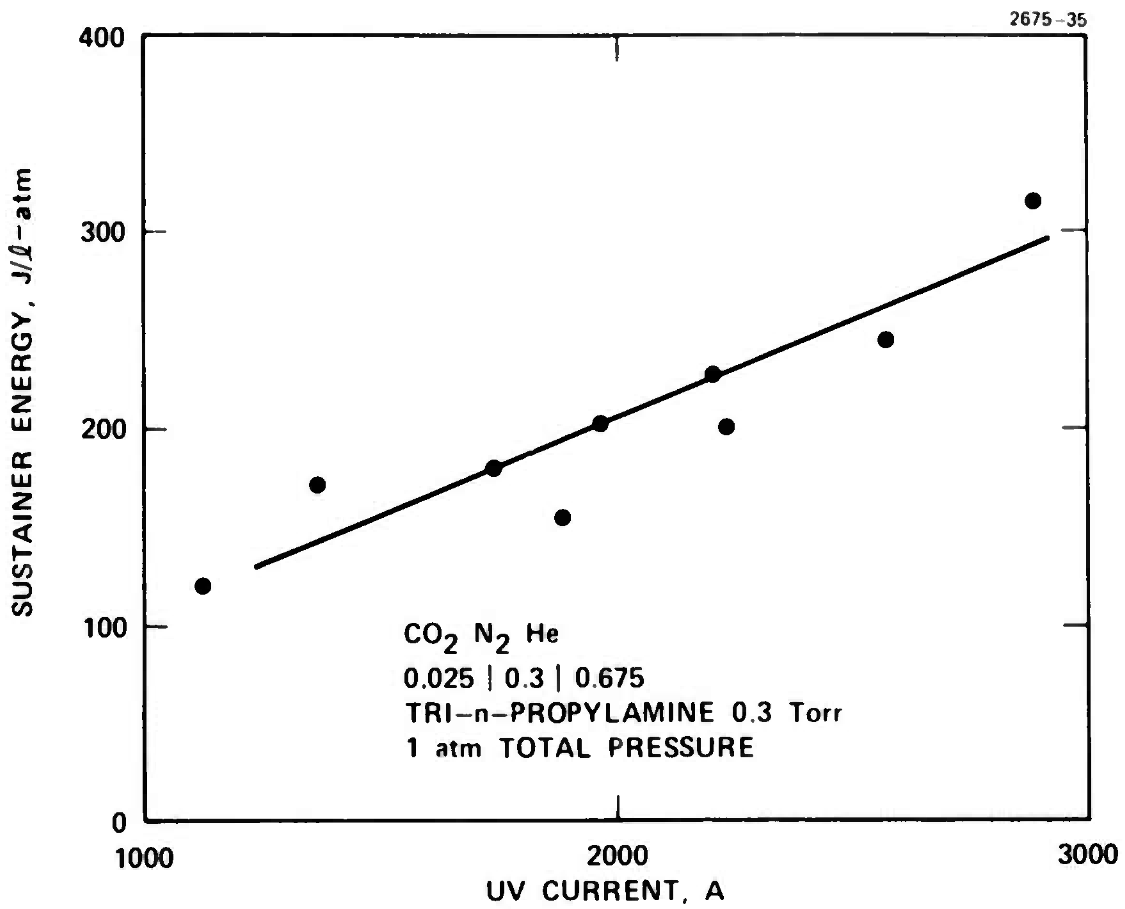

Fig. 4. Maximum input sustainer energy in J/l-atm as a function of uv current in amps.

deposited in the sparks and the sustainer discharge. Furthermore, experimental measurements directed toward alleviating this undesirable situation have demonstrated that a substantial decrease in the amount of radiated energy required can be obtained by the use of a type of "vacuum sliding spark" system (discussed below).

The effective mean free paths of the CO_2 and seed gas molecules have been evaluated from such data and summarized in Table 1. For a typical CO_2 mixture of 0.015 atm of CO_2 and 0.3 Torr of seed gas, the effective mean free paths are 11 cm and 20 cm, respectively, whereas the corresponding overall mixture mean free path is approximately 8 cm. As further confirmation for this projected mean free path, a characterization of the wavelengths responsible for the production of the observed photoionization of the added seed gases was undertaken. The results of such tests indicated that the observed dense plasma was produced by radiation with wavelengths between approximately 1200 and 1700 Å with more than 60% between 1500 to 1700 Å. Such a result can be explained by examination of the mean free path through CO_2 shown in Fig. 5. Because the ionization potential of tri-n-propylamine is 1720 Å, we conclude that single step photoionization is the production mechanism for the plasma. It is clear from the mean free path shown that below 1200 Å no radiation is transmitted through any reasonable size device that uses CO_2; thus we arrive at the limiting wavelengths obtained experimentally.

B. Small Signal Gain and Power Extraction

The gain and power extraction measurements were performed on a larger discharge device employing an improved source for the uv radiation. This source consisted of a two-dimensional array of cascaded arc discharges across a dielectric substrate (as shown in Fig. 6). (See second Semiannual Technical Report for a more detailed description.)

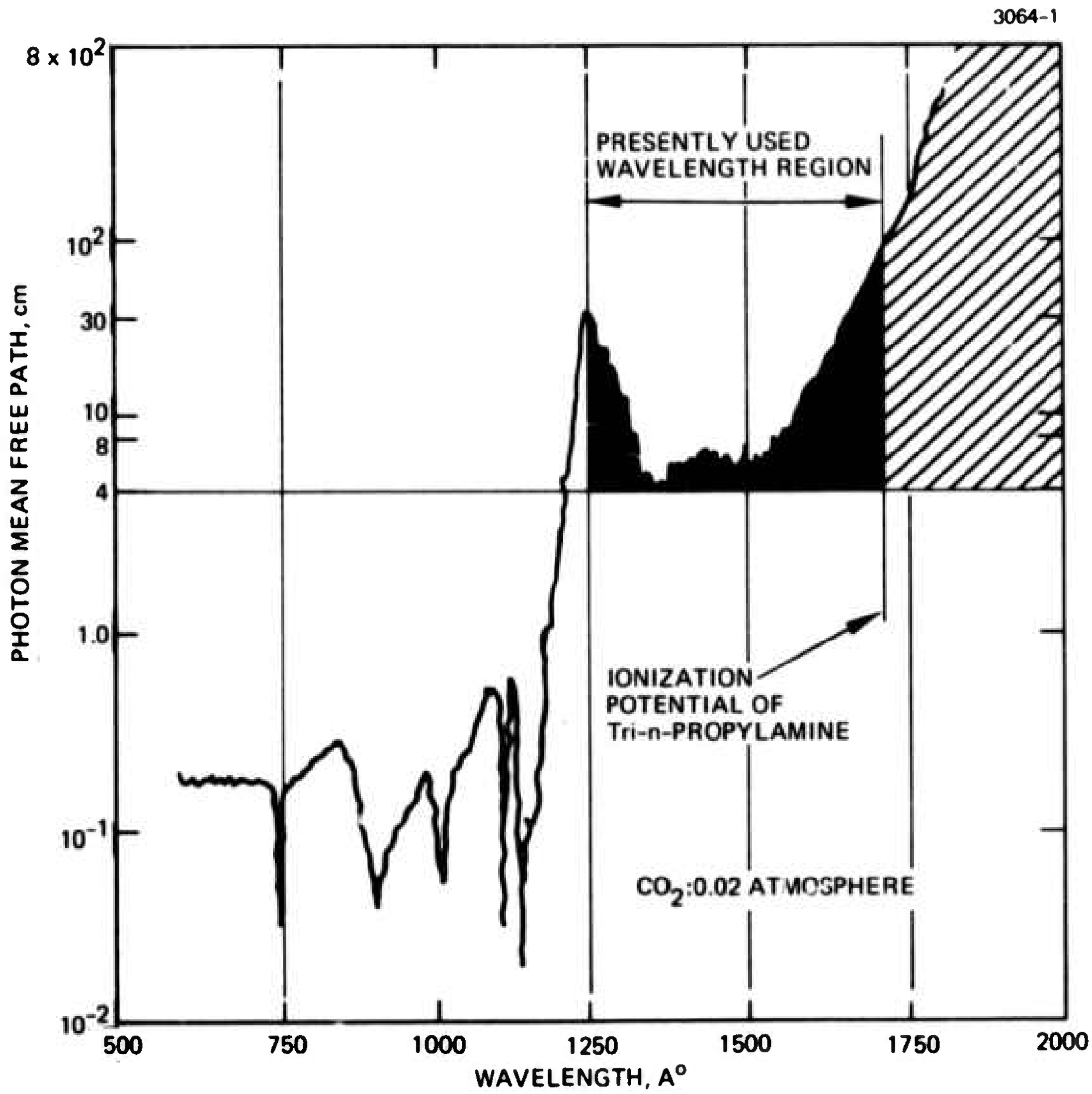

Fig. 5. Ultraviolet photon mean free path through CO_2 at 0.02 atm.

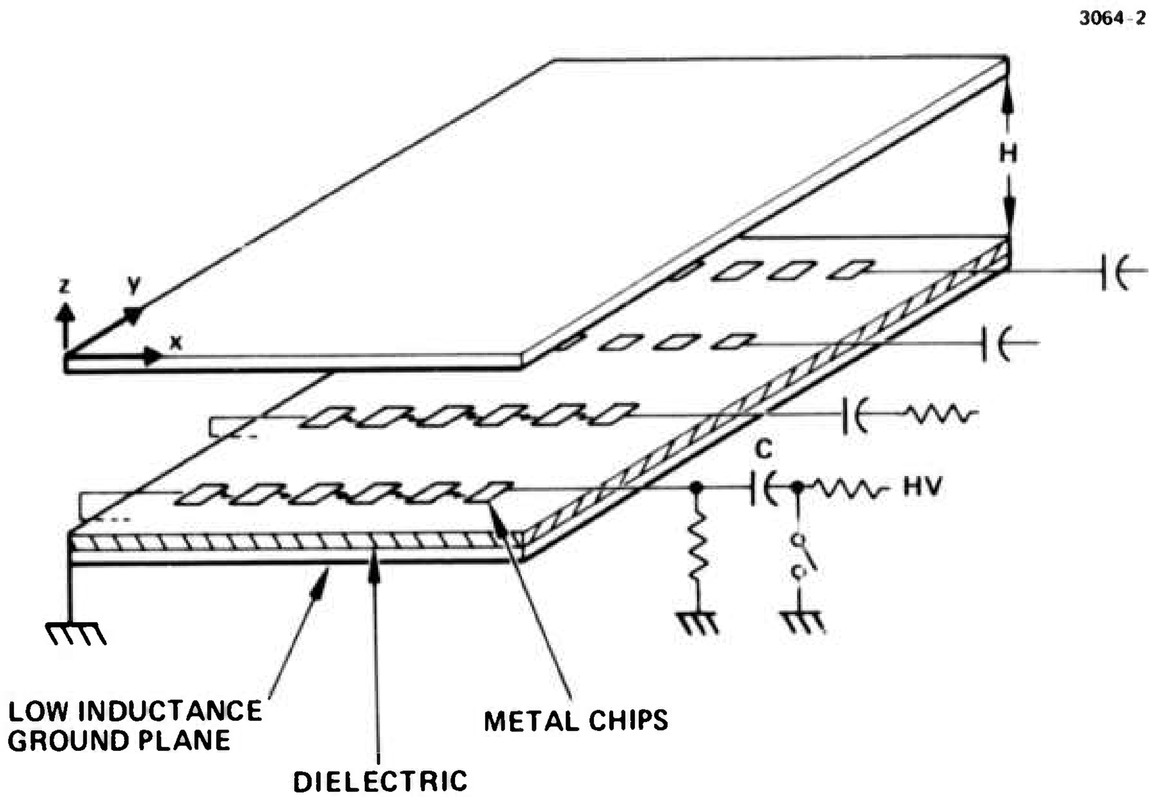

Fig. 6. Cascaded arc discharge system.

TABLE 1

Measured Effective Mean Free Paths of CO_2 and Seed (tri-n-propylamine) Gas

Molecules	Effective Mean Free Path[a] cm-atm
CO_2	0.16
Tri-n-propylamine	8×10^{-3}
[a]Typical mixture of 1 atm: CO_2:N_2:He:seed gas 0.02:0.3:0.7:0.004.	

T1195

To test the feasibility of this cascaded arc discharge source to uv sustained plasma conditioning, a medium volume ($2.5 \times 15 \times 50$ cm^3) test device was constructed from an existing laser testbed. This device had a Bruce profiled cathode located 2.5 cm from a flat mesh anode. Brewster angle windows were employed for use with external laser optics which consisted of a 4.5 m total reflector and a 20% transmitting dielectric coated output mirror.

Figure 7 gives typical current traces for the cascaded arc circuit and the sustainer plasma discharge obtained in a uv sustained mode. Figure 7(a) was obtained at an $E/N = 1.7 \times 10^{-16}$ V-cm^2 and Fig. 7(b) at an $E/N = 1.85 \times 10^{-16}$ V-cm^2. For the higher E/N the discharge is terminated by an arc occurring at approximately 22 μs into the pulse. Also, for the arc circuit, ringing occurs indicating that even though this uv source is more efficient there is a certain degree of impedance mismatch because of unavoidable circuit inductance.

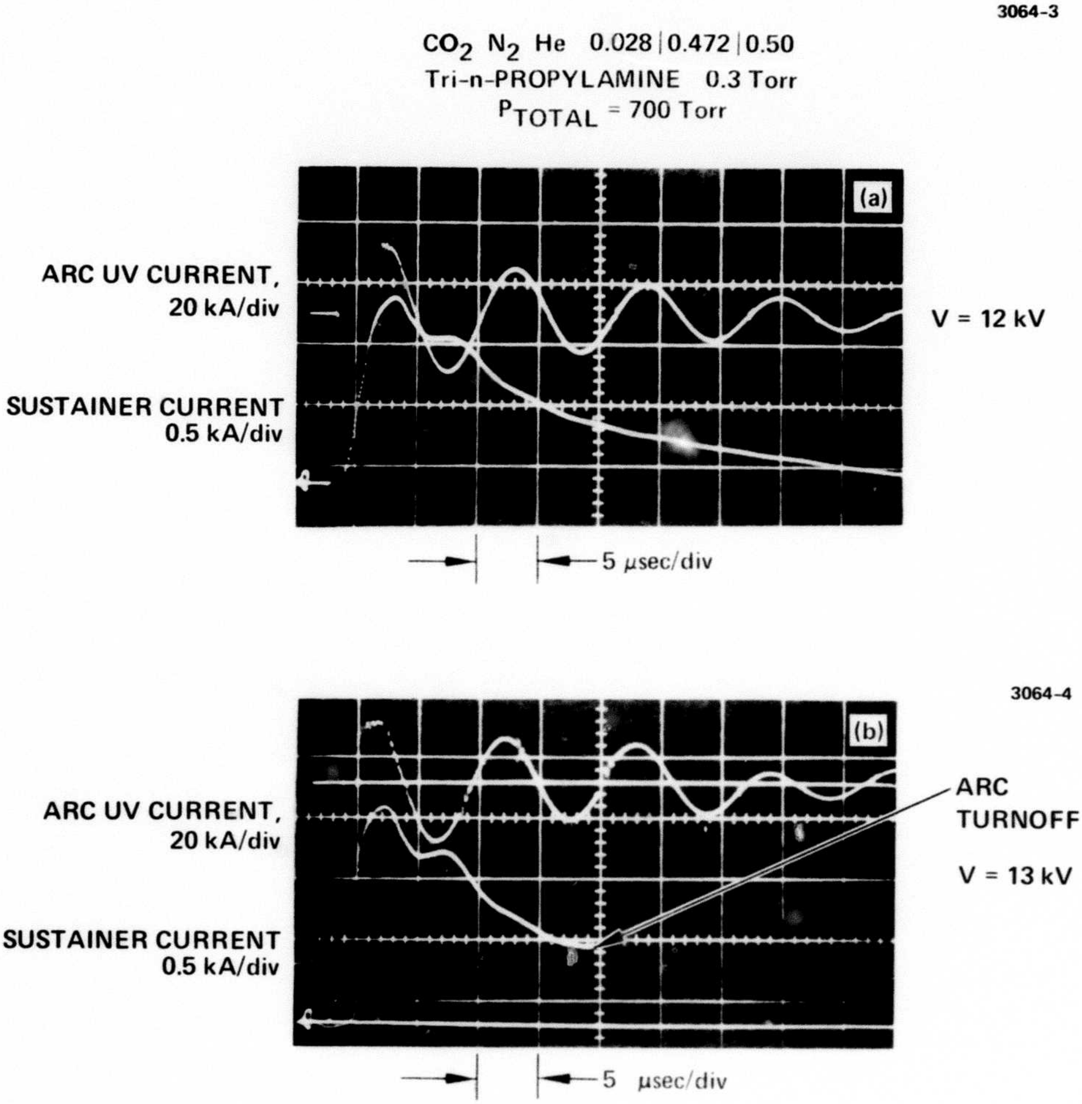

Fig. 7. Sustainer current and cascaded arc discharge current waveforms.

The energy input to the discharge was calculated by integrating the area under sustainer current curves such as these and then multiplying by the dc bias voltage. For the results of Fig. 7 this corresponds to about 350 J input which was the maximum value obtained for all cases run. By operating at higher bias voltages, arcing occurred much earlier in the pulse and hence led to the attainment of smaller input energies. The calculation of energy density depends on the discharge volume (which at this time has not been determined with a high degree of accuracy). However, taking the physical size of the electrode of 15 cm by 50 cm as the discharge area we find that an input energy density of 200 J/l-atm has been obtained for the above case.

The small signal gain was also measured for various mixtures, bias voltages (E/N), and position. A typical gain waveform is shown in Fig. 8. This trace was obtained at a point of 3.5 mm from the mesh anode, position 1 (see Fig. 9 for orientation), which corresponds to a location approximately 2.5 cm from the cascaded arc discharge uv source. From this trace the arrival of the acoustic disturbance from the uv source to the point where the probe laser is located is evident. The gain is observed to rise continuously throughout the pulse.

The gain distribution across the gap spacing was measured for various bias voltages. The results for a CO_2, N_2, He 0.028/0.472/0.50, 0.3 Torr tri-n-propylamine mixture are shown in Figs. 10 and 11. In Fig. 10 the gain as a function of bias voltage for the five probe positions is given. The gain varies in a nearly linear manner except for the position nearest the cathode where the gain begins to level off with increased voltage as observed in e-beam pumped systems.[3] In Fig. 11 the gain as a function of position for three bias voltages is given. We see here that the gain increases, as opposed to decreasing, as the distance from the uv source

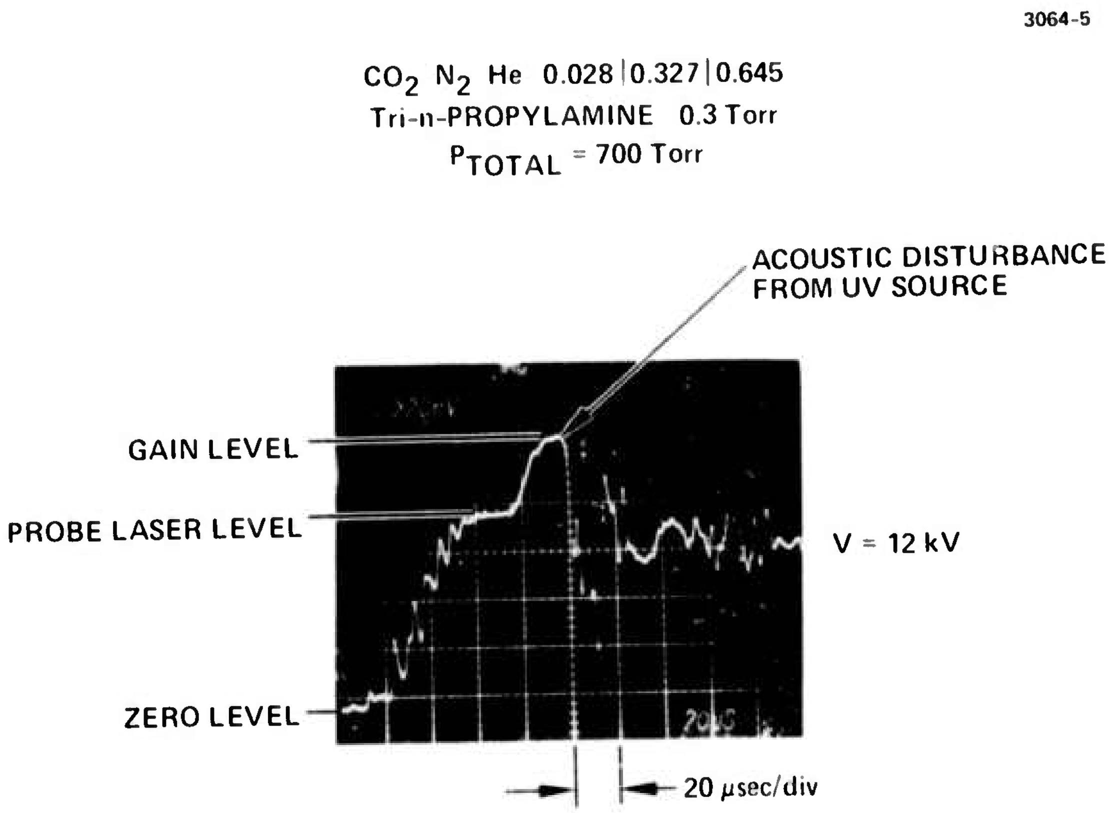

Fig. 8. Small signal gain waveform at position 1.

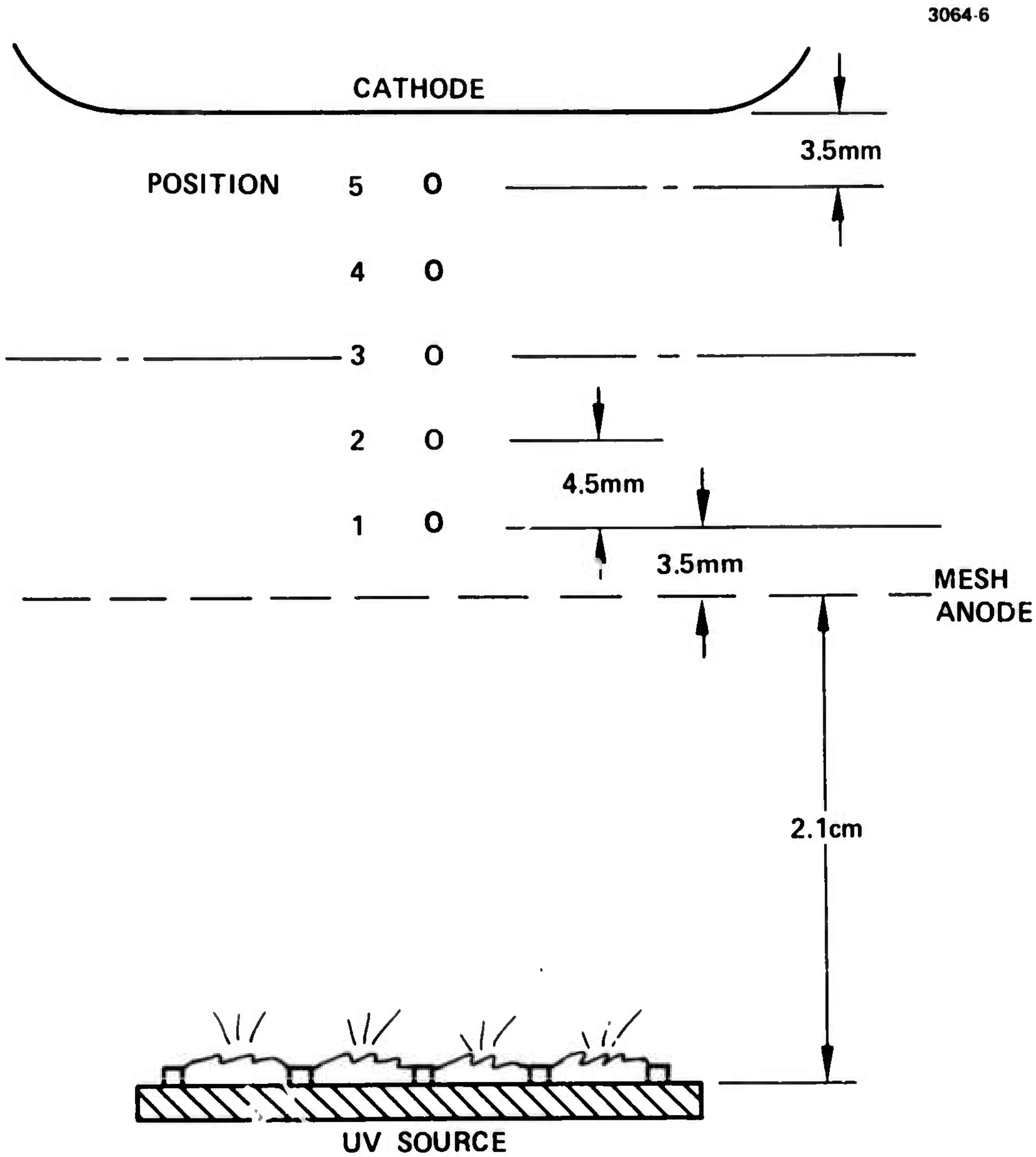

Fig. 9. Continuous wave probe laser positions.

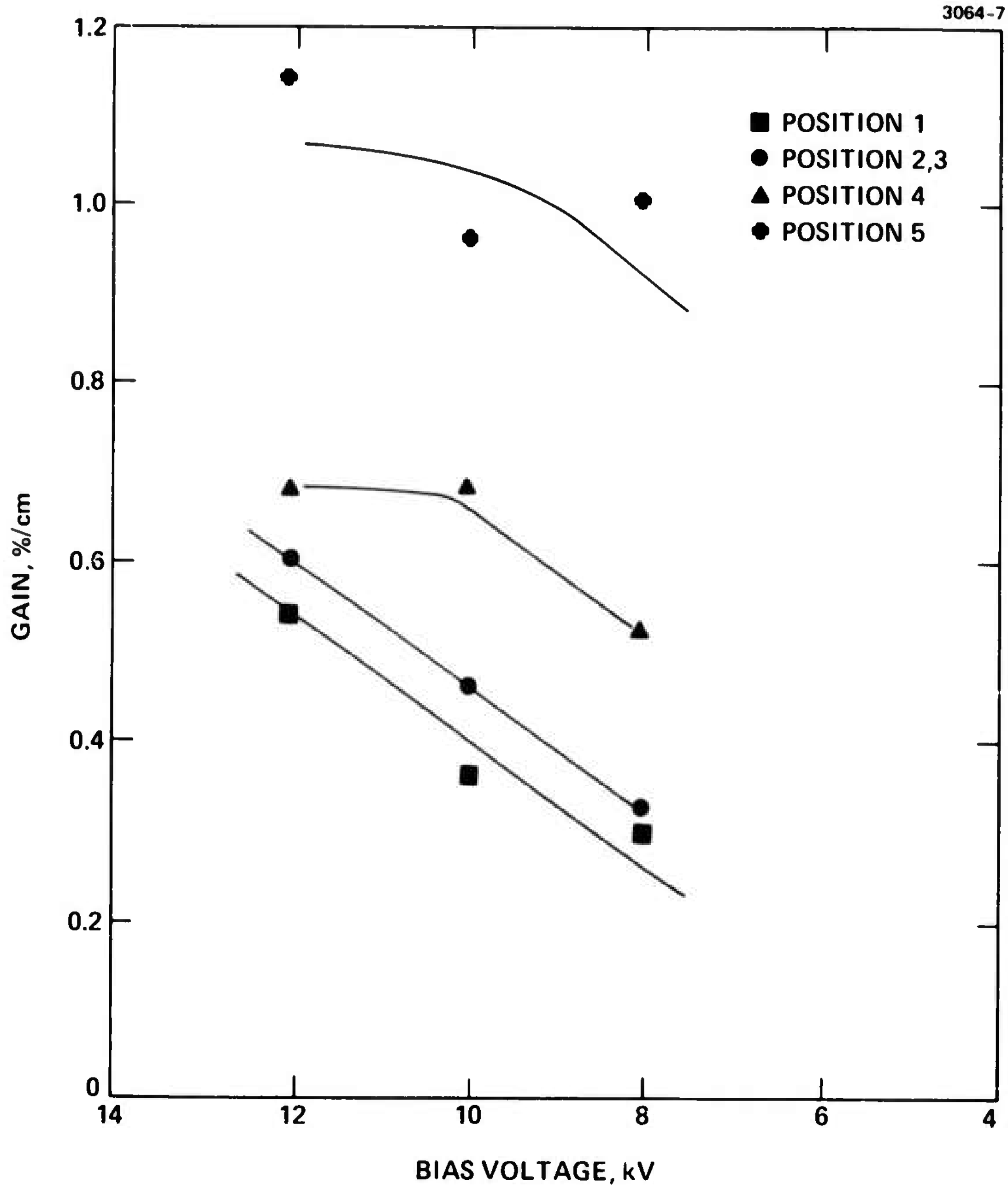

Fig. 10. Small signal gain as a function of bias voltage for 5 positions.

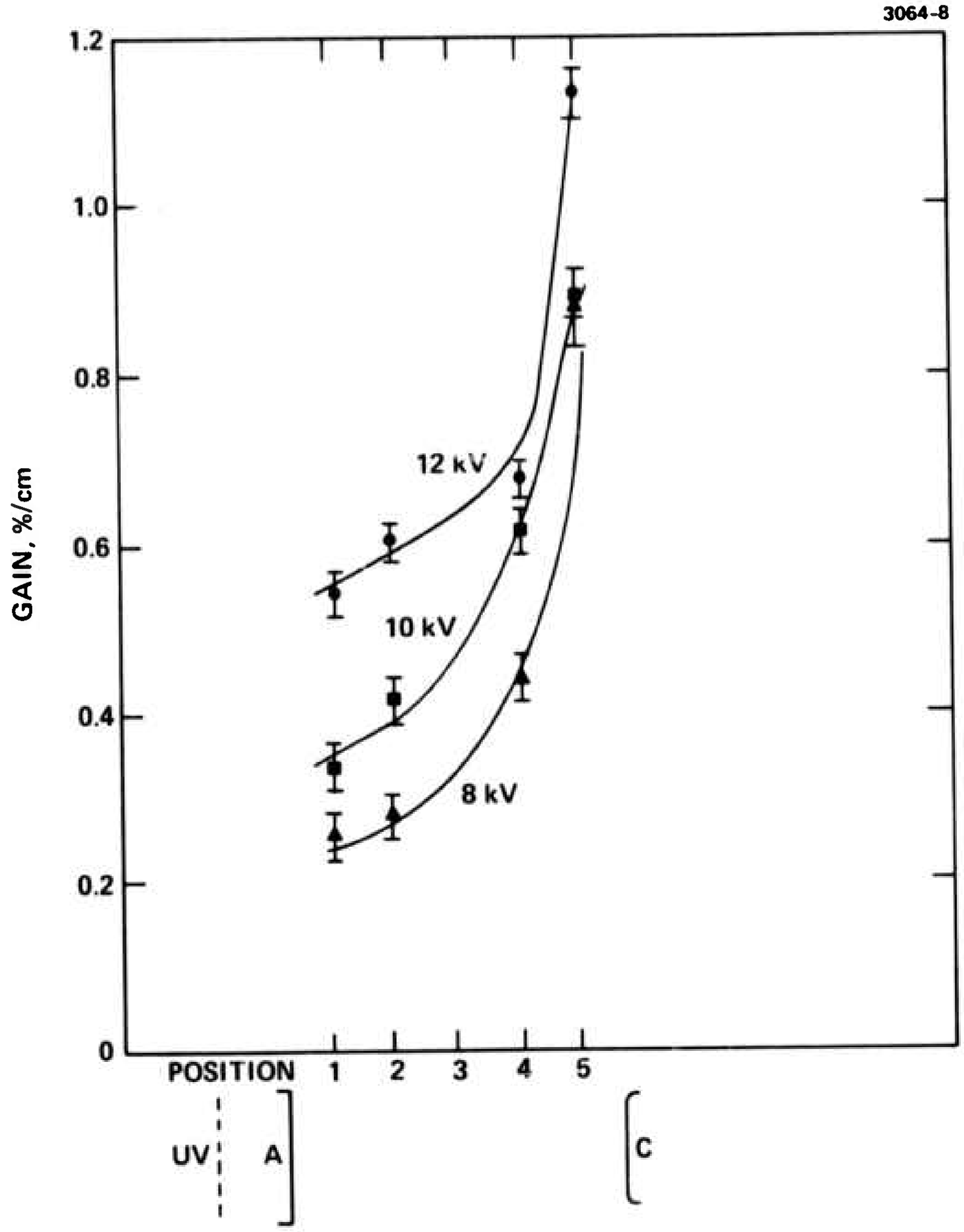

Fig. 11. Small signal gain as a function of position for various bias voltages.

increases. These results are indicative of the field strength increasing to maintain constant current, as n_e decreases moving away from the uv source, and thus rising to a value where possibly some local avalanching by the seed gas is occurring. In addition, the much higher gain near the cathode is a typical result seen for gain behavior in the cathode sheath region.[4] To indicate the very different nature of the gain waveforms near the cathode, the results obtained at position 5 are given in Fig. 12. Figure 12(a) is for 12 kV bias voltage and shows maximum pumping at the beginning of the pulse, because of the much higher n_e levels than obtained at position 1, and subsequent heating of the lower laser level during the remainder of the pulse (see Fig. 8). Figure 12(b) is for 8 kV bias voltage, and thus, much lower n_e levels, and shows pumping throughout the pulse duration but at a rate much lower than the case shown in Fig. 8 which was for 12 kV bias voltage.

Extensive measurements of laser output were made using a stable cavity arrangement and a Hadron Model 117 calorimeter. The measurements consisted of keeping the uv source energy fixed and varying the bias voltage (E/N) of the discharge and varying the gas mixture. Typical laser pulse shapes are shown in Fig. 13. The laser output shown in Fig. 13(a) and 13(b) corresponds to the cases discussed previously and shown in Fig. 7(a) and 7(b), respectively. Figure 13(a) gives a pulse with a multimode energy of 9.6 J and a pulse length of 37 μs. Figure 13(b) gives a pulse with a multimode energy of 12 J with a pulse that is terminated by an arc which occurs 22 μs into the pulse.

The near field burn pattern for the laser output is shown in Fig. 14. This pattern was obtained by using thermal chart recording paper. However, to determine the mode area more accurately, exposed photographic paper was used. This gave a slightly larger area than that shown. With the mode

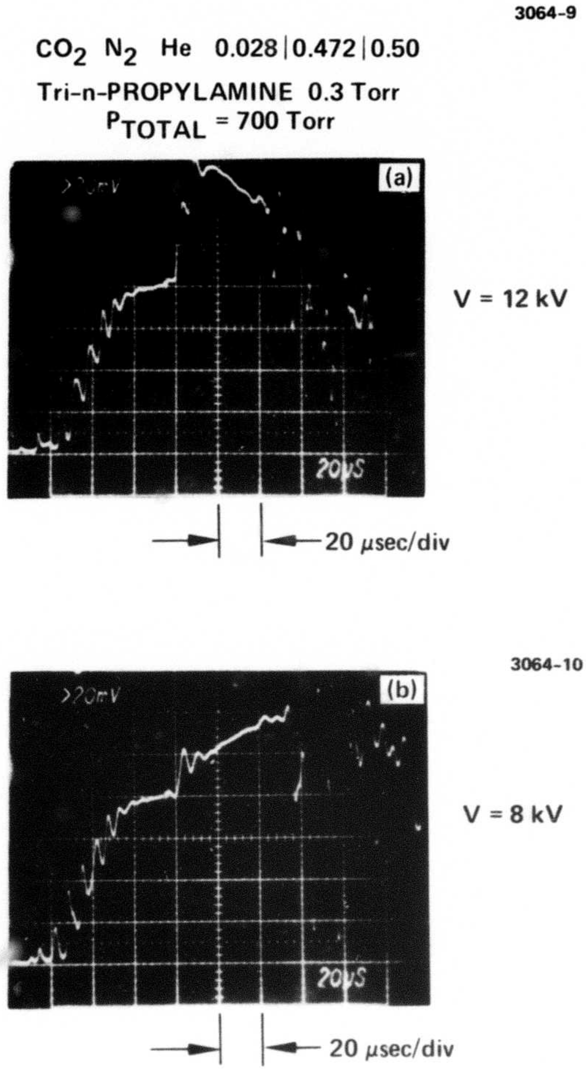

Fig. 12.
Small signal gain at position 5 for two bias voltages.

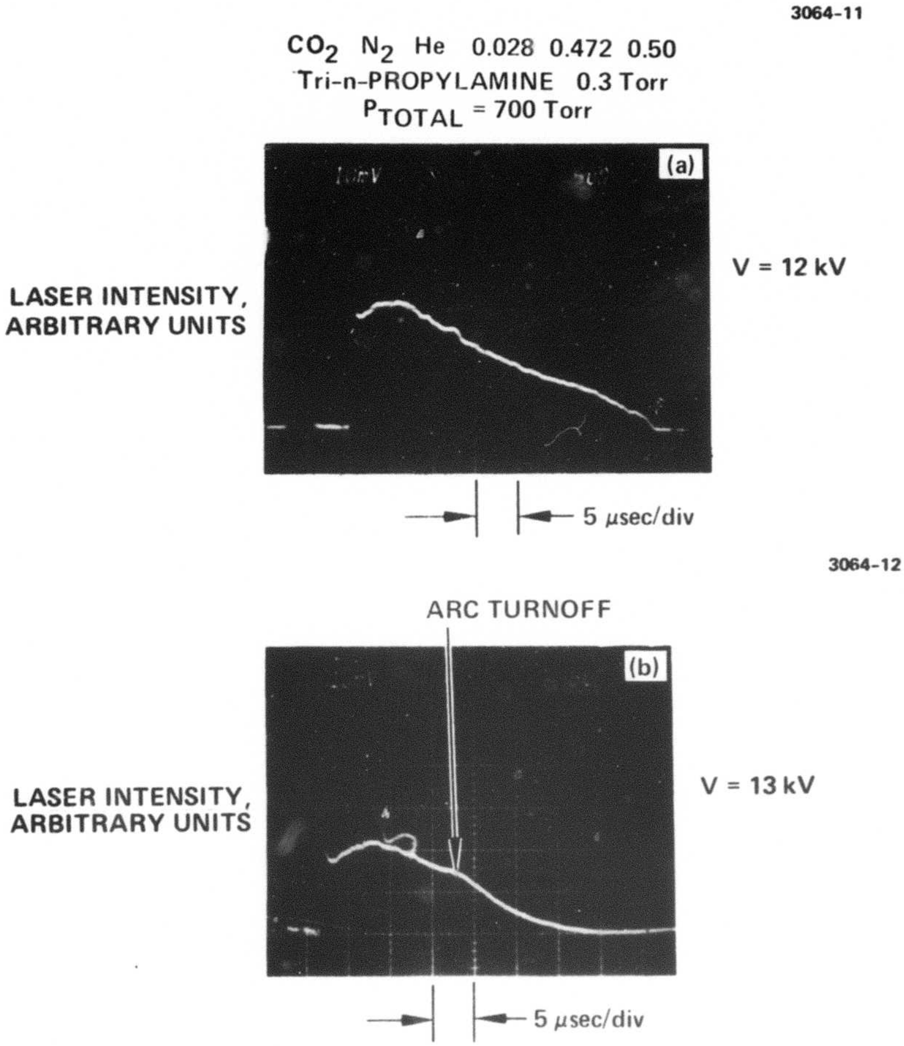

Fig. 13. Laser pulse shape.

volume established in this manner the laser output energy density can be determined. For the 37 μs pulse of Fig. 13(a), 47 J/l-atm was obtained, and for the shorter pulse (≈29 μs) of Fig. 13(b), 61 J/l-atm was obtained.

To indicate a typical variation in output with E/N, Fig. 15 gives such results for three CO_2:N_2:He, tri-n-propylamine mixtures. The fact that the output is lower at the largest E/N for the higher CO_2 concentration case results from an arc which occurred early in the pulse and lowered the obtainable input energy.

To calculate the electrical-to-optical conversion efficiency the input energy density is required. Using the estimated 200 J/l-atm value discussed previously we find that an efficiency of about 20 to 25% is obtained.

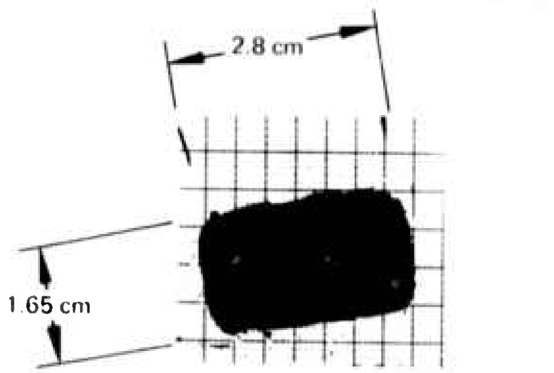

Fig. 14.
Near-field burn pattern.

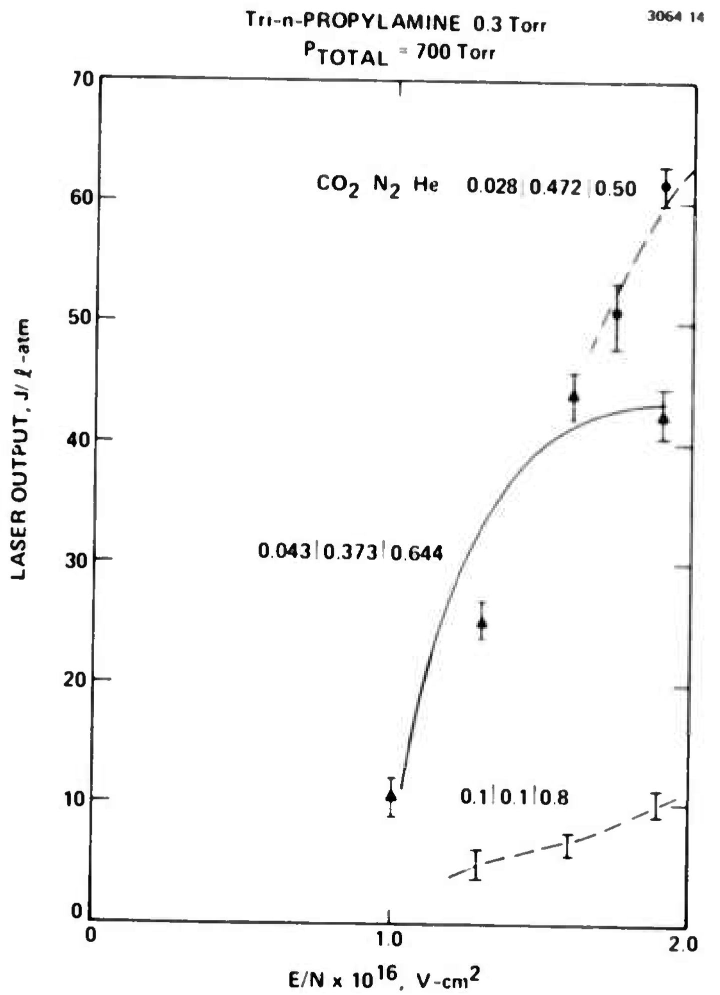

Fig. 15. Laser output as a function of E/N.

III. LARGE SCALE DEVICE STUDIES

During the last reporting period, construction of the large scale device was completed. The individual components were checked out and initial testing of the complete system was undertaken. In this section a detailed description of the device, together with the results of the initial tests will be given.

A. Device Configuration

The general concept of the device is that of a large vacuum chamber in which Bruce contoured electrodes are housed. A high energy (up to 50 kJ), 80 kV, dc storage bank is used to provide the necessary bias voltage to the electrodes. The uv source, which is the crucial element in the device, is located behind each electrode and irradiates the discharge volume through mesh screens that are wrapped around the electrodes.

The general layout of the laboratory in which the large scale device is located, is shown in Fig. 16. In this photograph we see the large vacuum chamber which houses the electrodes, the gas handling system, and the control console; Figure 17 shows one electrode installed in the vacuum chamber viewed from a direction looking toward the mesh screen. The screen is an approximately 50% transmitting stainless steel mesh through which the uv radiation passes. The next photograph (Fig. 18) shows the mounting of the uv source energy storage bank in relation to the electrode and uv cascaded arc discharge source (one bank for each electrode). The uv source energy bank is located in this manner to minimize wire lengths and hence loop inductance, which is critical to obtaining the maximum delivery of the stored energy to the uv arcs.
manner to minimize wire lengths and hence loop inductance, which is critical to obtaining the maximum delivery of the

M10470

3481-9

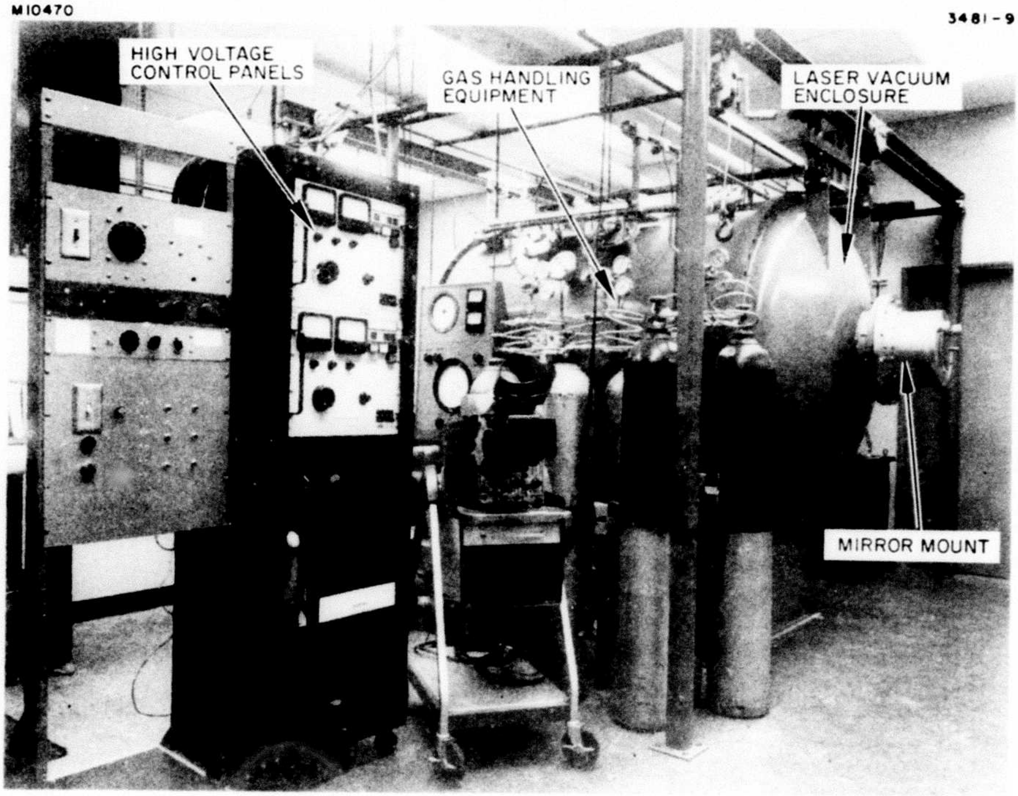

Fig. 16. Device and associated equipment.

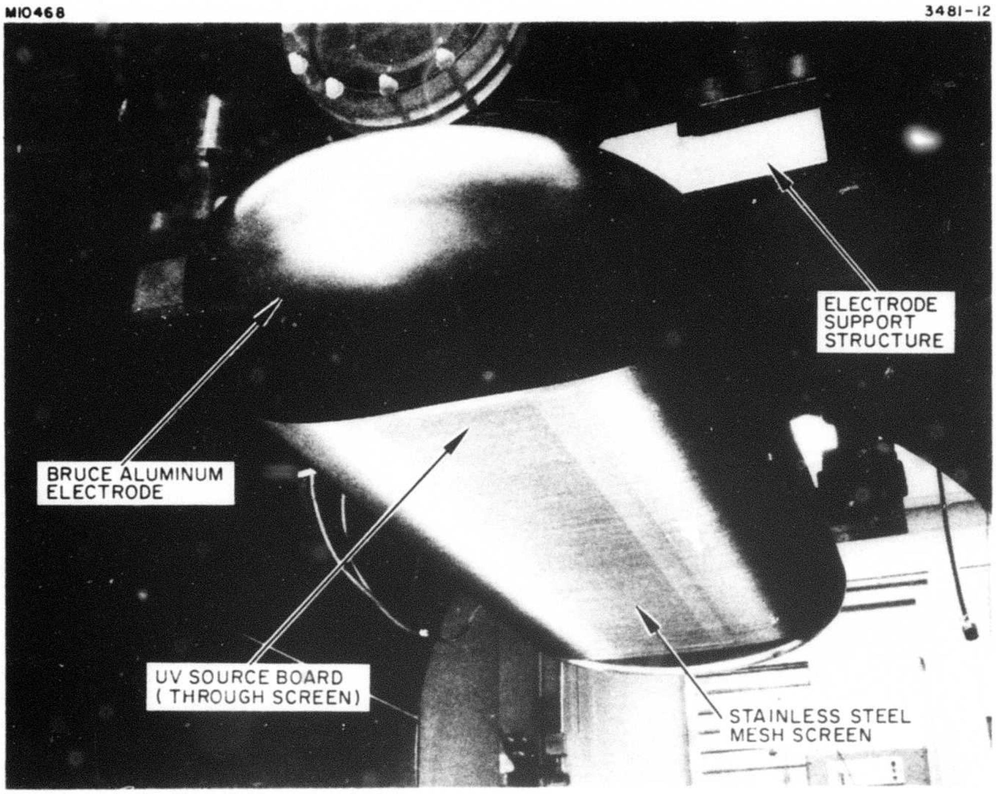

Fig. 17. Upper electrode.

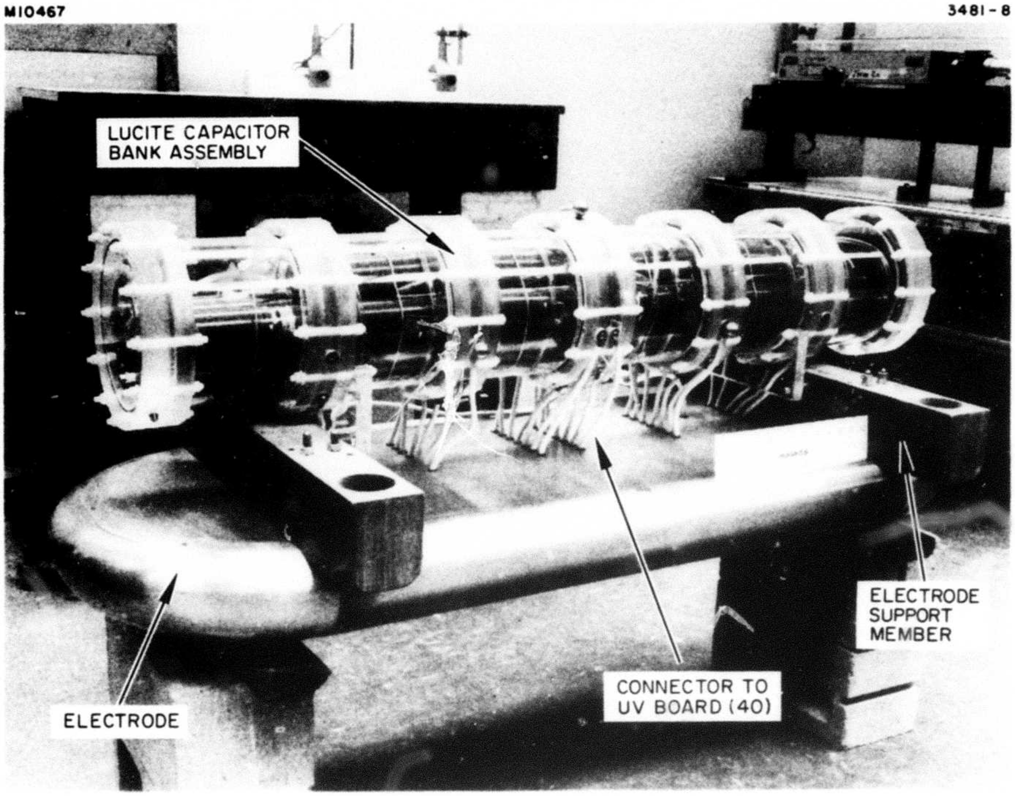

Fig. 18. Ultraviolet source capacitor bank assembly.

The uv source itself is shown in Fig. 19. The source consists of cascaded arc discharge boards with approximately 40 rows of arcs, each row having copper chips 3 mm x 3 mm along the 100 cm discharge length. Each row is energized by a separate 0.1 μF, 25 kV low inductance capacitor (shown installed in the previous figure). Figure 20 depicts the assembled discharge device. Shown are the N_2 spark gaps which fire the uv source capacitor banks, the spray bars which ensure proper gas mixing, and the electrode support columns and spacers which in the present configuration give a 6 cm electrode spacing.

To ensure proper mixing of the organic seed gas molecules (tri-n-propylamine) in this large volume device (2800 liters) an arrangement different than that used on the previous small scale experiments is employed. Here the seed molecule is injected into a flowing gas stream of N_2 immediately downstream of a sonic orifice ensuring complete breakup of the liquid into tiny droplets, vaporizing, and mixing as the stream enters the discharge chamber.

Finally, the electrical circuits employed are documented in detail in the second semiannual[2] report to which the reader may refer.

B. Preliminary Results

Initial operation of the device took place during this reporting period with the principal result that a maximum extraction energy of 115 J was obtained, in a configuration employing a 6-cm electrode gap spacing. This extraction energy corresponds to an energy density of 27 J/l-atm. We shall show below that information concerning the potential scalability and medium uniformity of the device can be obtained from an analysis of the output energy and mode volume obtained from these initial results.

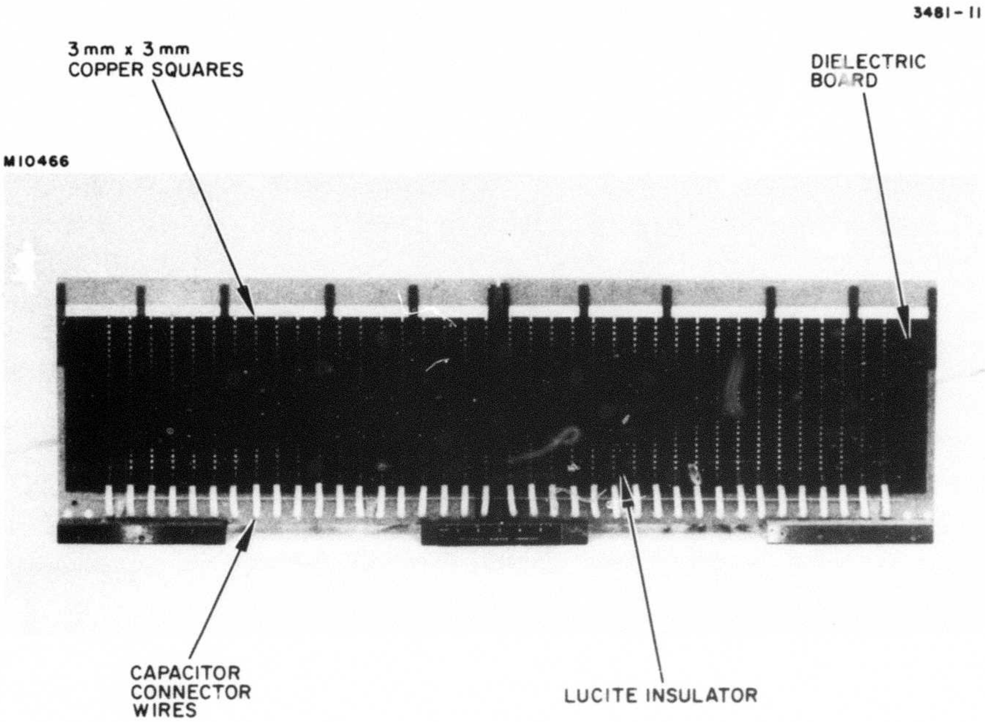

Fig. 19. Ultraviolet source boards.

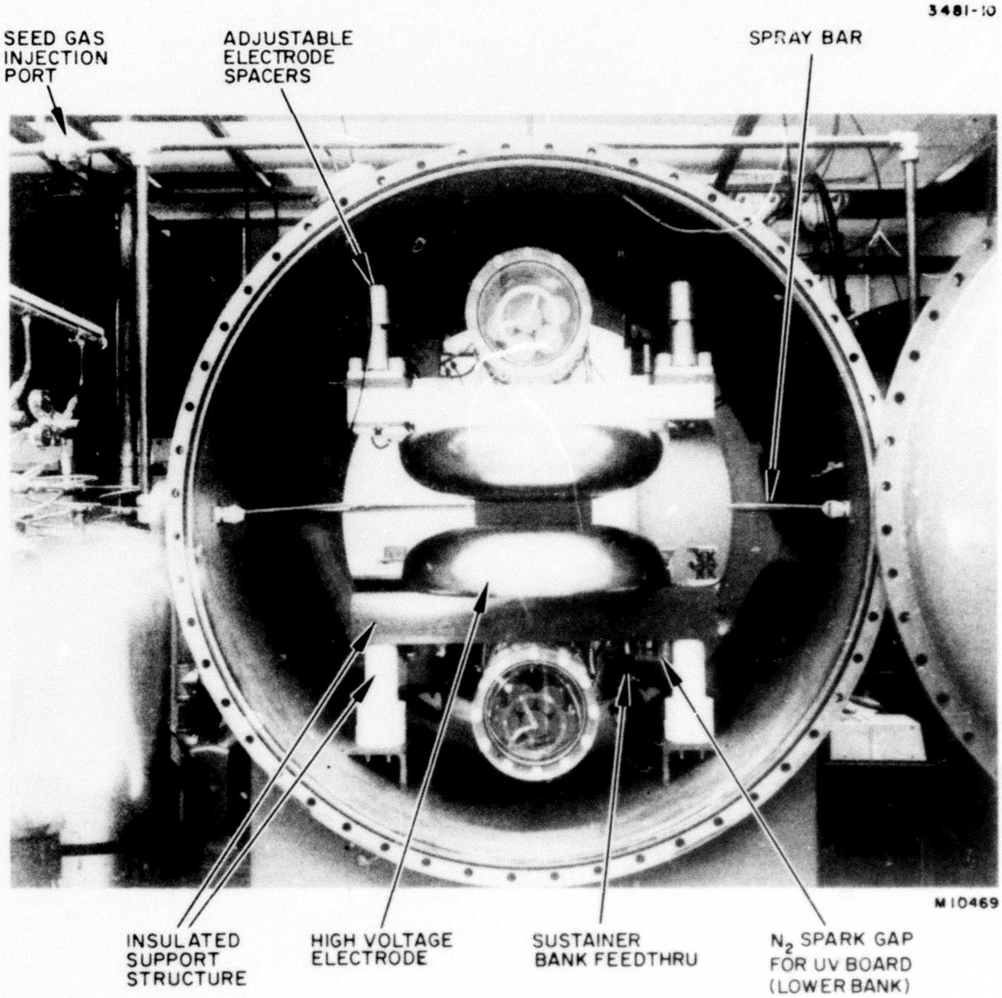

Fig. 20. End view of assembled device.

Before discussing the results, it is of interest to mention one experimental problem that arose during the investigation. This problem relates to the failure of the energy storage-bank crowbar system to operate consistently. The crowbar is used to remove the voltage from the sustainer electrode at a predetermined time after firing the uv source. This prevents the post-arcing phenomena typical with non-avalanche discharge devices. In Fig. 21 the relationship between the crowbar and the other components in the system together with the timing sequence is given. The failure characteristic was the inability to achieve proper timing. Noise from the uv source firing caused the crowbar spark gap to trigger at the beginning of the pulse, and if the spark gap pressure was increased it was not possible to trigger the spark gap at all. The circuit originally used is shown in Fig. 22 where the E.G.&G. TM 11A trigger transformer was used to trigger the spark gap. To solve these problems the function of the TM-11A was replaced with the circuit shown in Fig. 23. Here considerably more energy was available resulting in consistent triggering and further, the Schmidt trigger circuit incorporates an integrating feature which prevents the high-frequency noise signal from the uv source from causing a false trigger. With this arrangement the crowbar circuit operates as expected.

1. Energy Extraction Results

To extract laser energy a hole-coupled, stable cavity arrangement was used. The optical arrangement employed is shown in Fig. 24. A 6 in. diameter, 11 m radius, total reflector, together with a 6 in. diameter, flat, 25% hole-coupled mirror made up the internally mounted stable cavity. Each mirror was nickel plated, polished, and coated with silver-thorium fluoride. The beam upon leaving the vacuum tank passed at normal incidence through a salt flat to the outside. To measure total laser energy a fraction of the

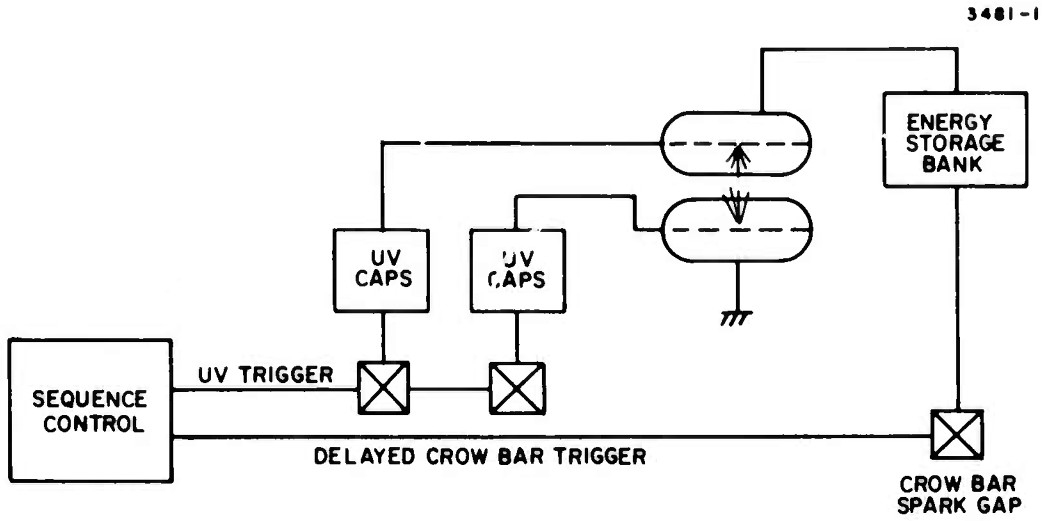

Fig. 21. Crowbar and timing sequency circuit.

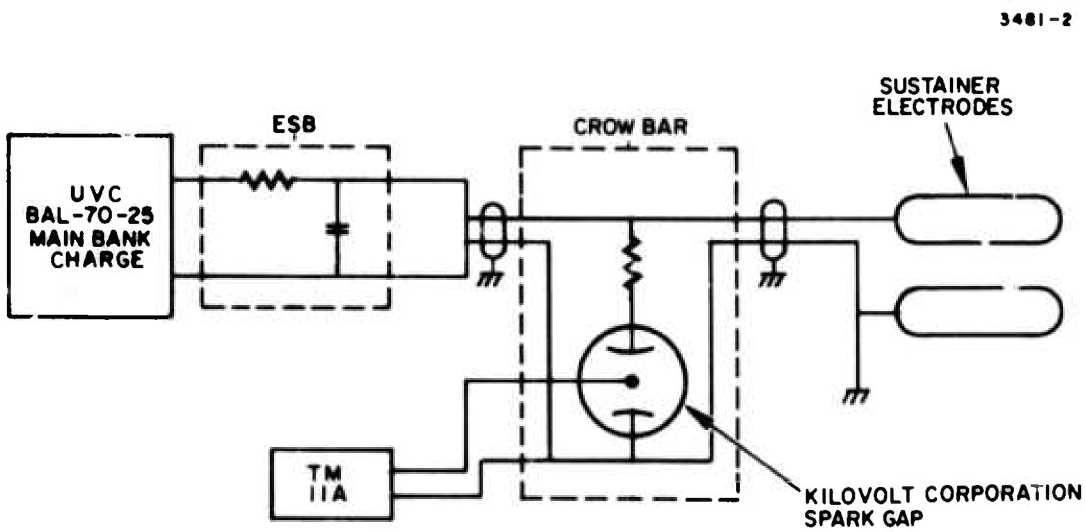

Fig. 22. Original crowbar circuit.

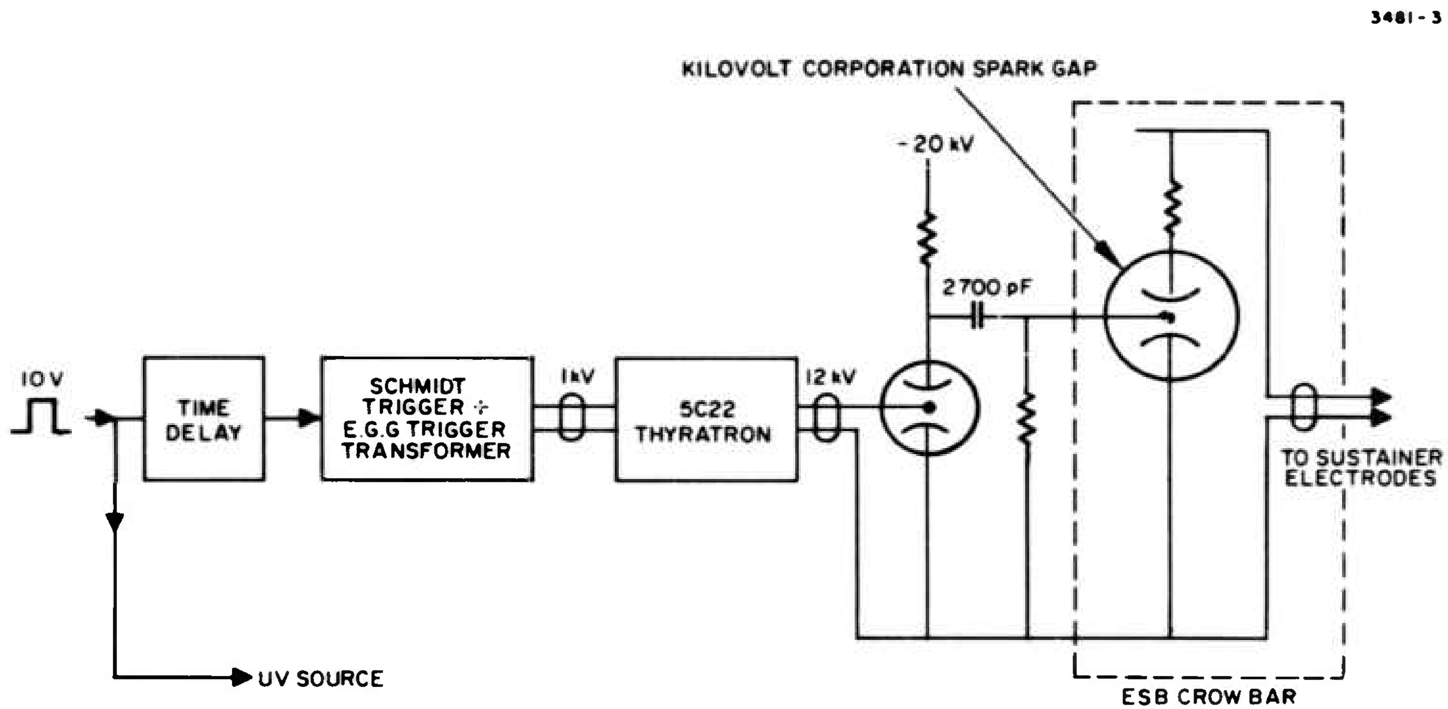

Fig. 23. Revised crowbar circuit.

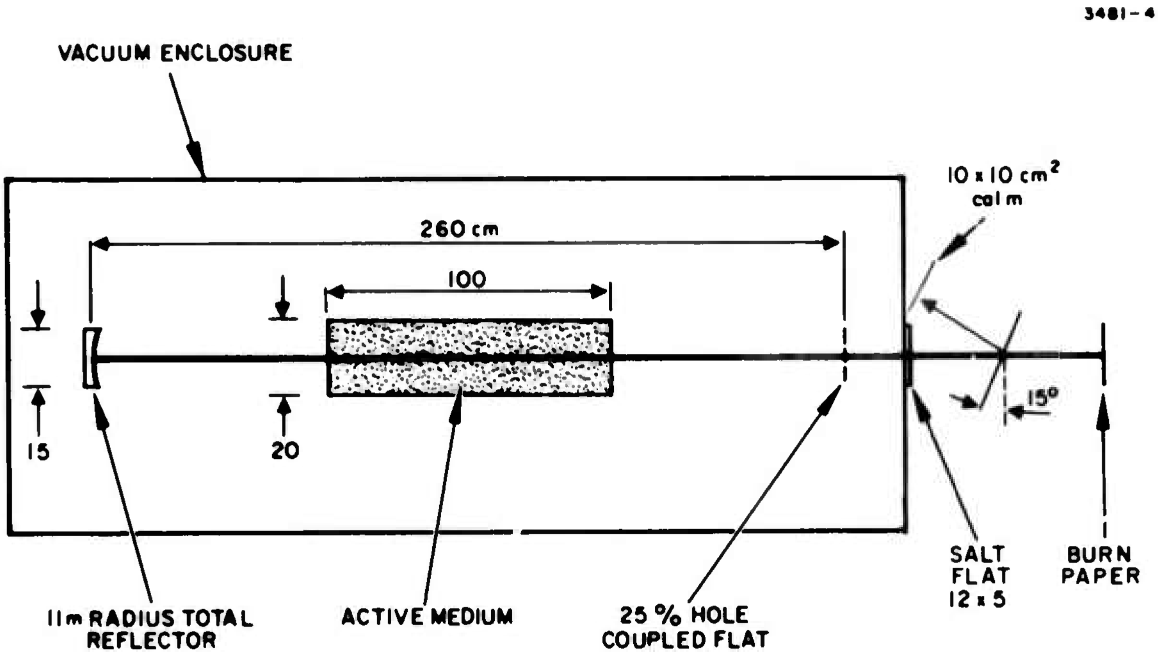

Fig. 24. Optical arrangement.

beam was reflected from a salt flat oriented at a known angle (15^{o} to the beam) and onto a calibrated calorimeter. Approximately 8% of the beam was intercepted by the calorimeter with the remainder transmitted through the beam splitter onto a piece of thermal chart recording paper to obtain a near-field burn pattern.

The calorimeter consisted of a 10 cm x 10 cm anodized aluminum flat plate and a massive reference plate. The beam impinged on the plate and was almost completely absorbed by the Al_2O_3 surface with the resulting temperature rise of the plate measured by a series of thermocouples attached to the back of the plate (relative to the massive reference junction) to determine the energy. The calibration of the calorimeter was determined in three ways: (1) by adding a known amount of heat in a pulsed mode to the plate, (2) by comparing directly with the results from a Hadron model 117 calorimeter, and (3) by calculation, knowing the thermal response of the anodized aluminum plate. The calibrations were in excellent agreement with a calibration factor of 13.5 μV/J obtained.

The output energy obtained in this manner for three different gas mixtures as a function of sustainer voltage is shown in Fig. 25. It is possible to conjecture from these preliminary results an important aspect related to the scalability of the device. This arises from the fact that, at least for these initial results, the output energy is the same for the 2.7% and 5% CO_2 mixture cases. We have determined previously (see Section II) that the uv photon mean free path is essentially determined by the CO_2 concentration in the mixture. Thus, the electron density and hence energy input depend on gap spacing as $n_e \propto \exp(-L/\lambda_{CO_2})$ (see Fig. 2), where L is the effective gap height and λ_{CO_2} is the mean free path at a given pressure of CO_2. Since the output energy, which is directly related to the electron density, remained constant when doubling the CO_2 concentration, this implies

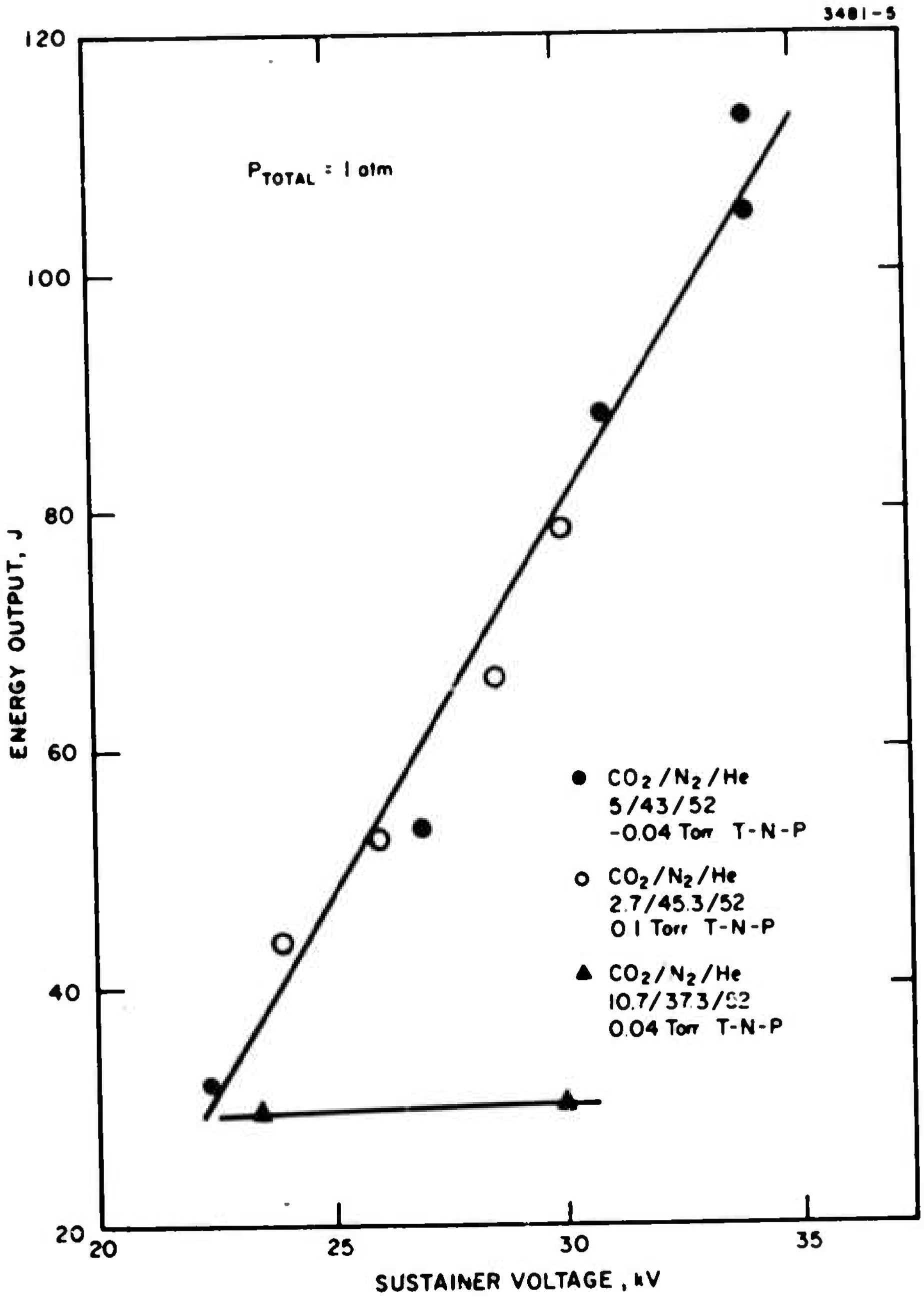

Fig. 25. Laser output as a function of sustainer voltage.

that the effect of the exponential falloff was insignificant. Therefore, we should be able to double the gap height and operate with a 2.5% CO_2 concentration and still obtain the same specific output energy. This follows from the ratio $L/\lambda_{CO_2} \approx LP_{CO_2}$. Therefore, (2L) (2.5%) = (L)(5%), where L in this case is 6 cm. At a spacing of 12 cm there is a total separation of the uv sources of 16 cm (each uv source is located 2 cm behind its electrode). This distance is consistent with the projected mean free path of 8 cm (16 cm for two sources). These results are preliminary in nature, however, and further data is needed to substantiate this result.

We also see from Fig. 25 that doubling the CO_2 concentration again to 10.7% results in a substantial decrease in power output. This indicates that the mean free path is certainly within the bounds expected.

From Fig. 25 we see that the maximum output obtained to date is 115 J. The near-field burn pattern for the 115 J case is shown in Fig. 26. Based on the mode volume calculated from this burn pattern, the output energy density is 27 J/l-atm. This is a significant result for these preliminary measurements, since it is only a factor of 1.5 below the optimized small-scale results.

2. Medium Characterization

Analysis of the active mode area of the laser burn pattern of Fig. 26 allows an initial characterization of certain features of the discharge medium. The smaller dimension of the burn pattern corresponds to the distance between the electrodes which in the present case is a nominal 6 cm. We see from the burn pattern that laser action occurs over only 5 cm out of the 6 cm possible. The reason for this is conjectured to be acoustic effects caused by the uv sources. Specifically, the uv source, when fired, produces a large acoustic disturbance which propagates into the region near

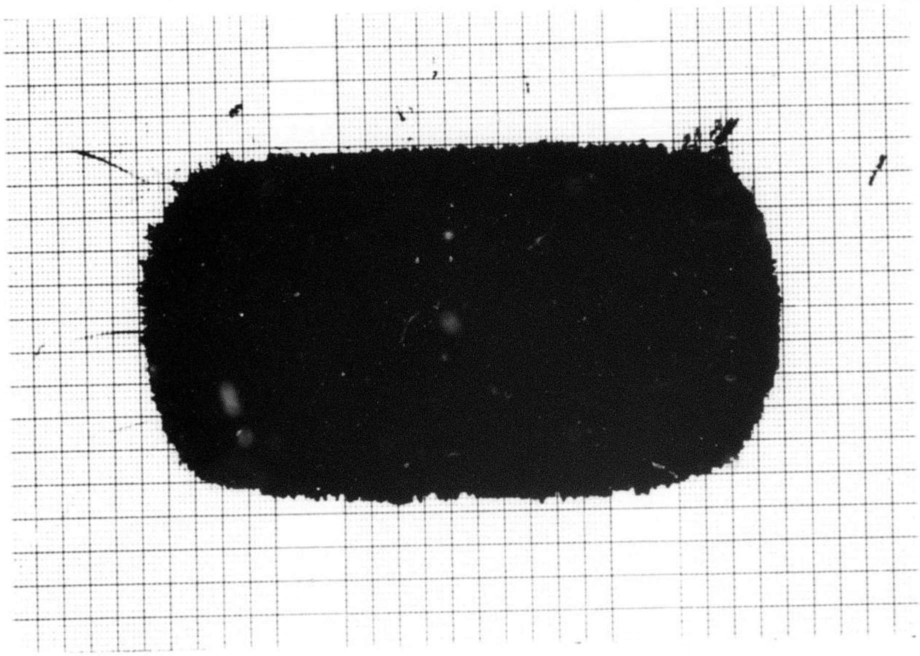

Fig. 26. Near-field burn pattern.

the electrodes. This distrubance would lead to large density gradients, possibly of a manitude sufficient to suppress laser oscillation in that region.

The larger dimension of the burn pattern corresponds to the discharge width which has an active uv source width of 20 cm. However, for these preliminary experiments use is not made of the full 20 cm active width because of the optical arrangement employed (see Fig. 24). The hole coupled output mirror has a 15 cm diameter which represents the first width aperture and the salt flat on the vacuum enclosure, through which the beam passes to the outside, has a width of 12 cm which represents the limiting aperture for the beam. The burn pattern shows that the active width is only about 9 cm. This indicates that the pumping in the outer regions of the discharge is not sufficient to produce enough gain to overcome the losses occurring there. It is expected that the electron density, hence gain, would fall off at the edges of the uv source based on previous calculations (see second semiannual report Fig. 17)[2], but it is surprising that the fall-off would be sufficient to reduce the width to 9 cm. This is a signficant effect and requires further detailed measurements of the spatial distribution of small signal gain coupled with medium homogeneity measurements to understanding conclusively the cause. These measurements will be undertaken in the next reporting period (see Section IV).

3. Laser Efficiency

Having established encouraging specific energy performance, a quantity of prime interest is the efficiency of the system. However, at the present time calculation of this efficiency is not possible because of difficulties in obtaining consistent measurements of the total current into the discharge. When the device was disassembled for minor repairs, evidence was found that an arc-over had been occurring from one of the sustainer electrodes to a portion of the

vacuum tank creating a secondary path to ground for the sustainer current. Thus the current sensing unit was recording only a portion of the total discharge current. This problem has been corrected by redesign of the insulator assembly. Efficiency measurements will be carried out during the next contract period.

IV. SUMMARY AND FUTURE PROGRAM PLAN

A. Summary of Results

Significant results obtained on the contract to date are listed below:

- Demonstration of a 37 μs laser output pulse with an energy density in excess of 45 J/l-atm in a 1 atm CO_2 laser mixture in a uv sustained mode.
- Characterization of small signal gain, both temporally and spatially resolved, using a medium volume device (2.5 x 15 x 50 cm^3). Values between 0.5 and 1.0%/cm are typical.
- Demonstration of a more efficient uv source on the 2.5 x 15 x 50 cm^3 device.
- Calculation of expected electron number density spatial variation for the large-scale device with variations up to only 50% expected.
- Construction of the 20 x 20 x 100 cm^3 device completed.
- Preliminary measurement on the large scale device, with a 6 cm electrode gap, of 115 J output, corresponding to 27 J/l-atm energy density.

B. Program Plan for Large Scale Device

Originally, it was planned to have completed, in addition to the extraction measurements discussed above, medium homogeneity and small signal gain spatial distribution measurements during the present reporting period. However, because of delays in receiving crucial pieces of hardware for the device from various vendors these measurements have been delayed. Because medium quality is an essential element

Preceding page blank

of any device characterization it has been decided, in conjunction with the contract monitor, that a major portion of the follow-on program consist of medium homogeneity, small signal gain, and stable and unstable resonator power extraction measurements. The objective of these measurements will be to fully evaluate the scaling characteristics of the uv sustained discharge concept.

The follow-on program plan is shown in Fig. 27. Task 1 is the measurement program on the large scale device discussed above. This plan follows the general scheme of (a) obtaining more detailed extraction measurements employing hole-coupled output mirrors. A 25% coupling was used for the results discussed in Section III. In addition, a 9% coupler is available which will be used in determining optimum output coupling for the unstable resonator experiments, (b) measure the small-signal gain spatial distribution and medium homogeneity with particular emphasis on the mode volume problem discussed in the previous section, and (c) with scaling limits established, that is, with the useful gap height and discharge width known, an unstable resonator will be designed and constructed to fully utilize this discharge area. Extensive tests will be performed to determine the maximum single shot output from the device.

C. CW UV Source Development

Tasks 2 and 3 deal with a proposed extension of the uv sustained concept from the present single shot capability to a truly cw operation. Under these two tasks the research, design and testing of a uv source configuration for cw operation will be performed. In addition, the problems associated with implementing such a source on a flowing system will be addressed.

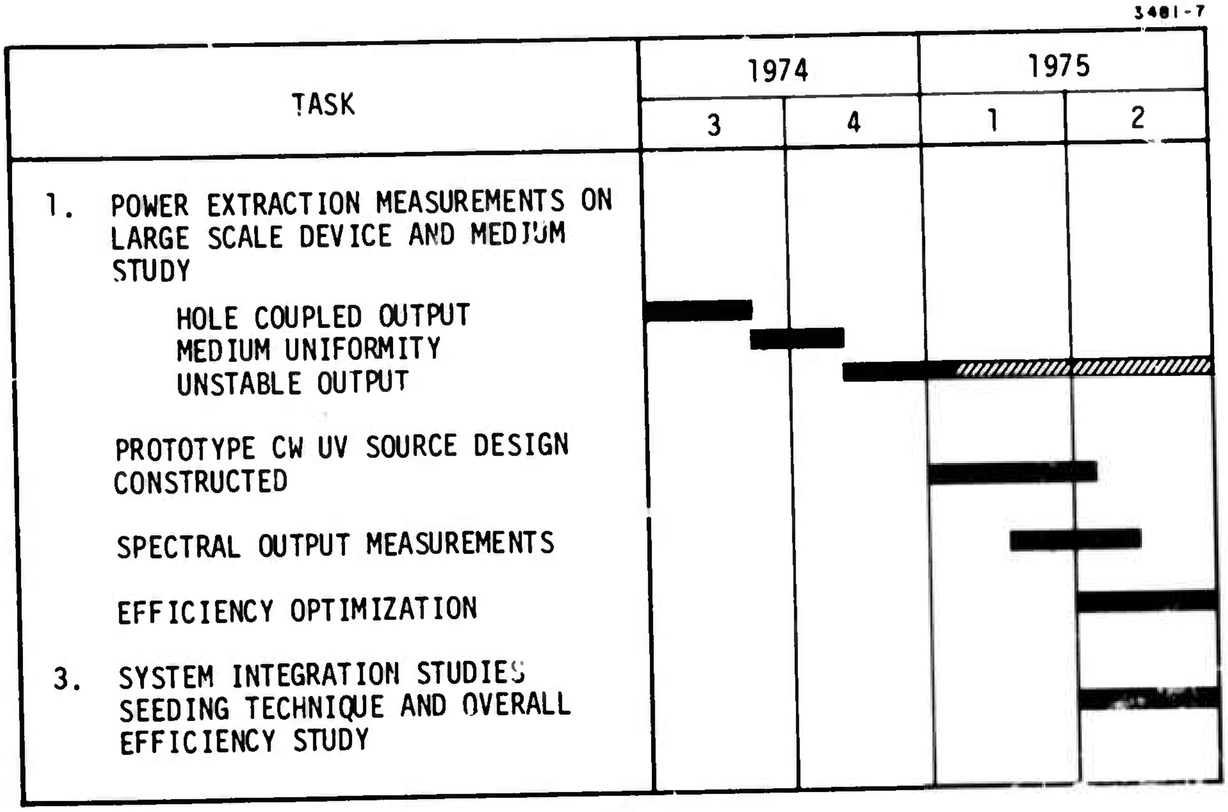

FOLLOW-ON PROGRAM PLAN

Fig. 27. Fol n program plan.

Since this subject does not relate directly to the material presented in this report its content will be discussed further in a later report. (Also see Technical Proposal 74M-4592/D2468, March 1974).

REFERENCES

1. R.C. Lind and J.Y. Wada, "Investigation of UV Photoionization Sustained Discharge for Gas Lasers," First Semiannual Technical Report, Contract N00014-73-C-0287, Hughes Research Laboratories, Malibu, California (173).

2. R.C. Lind, W.M. Clark, and J.Y. Wada, "Investigation of UV Photoionization Sustained Discharge for Gas Lasers," Second Semiannual Technical Report, Contract NO-014-73-C-0287, Hughes Research Laboratories, Malibu, California, March 1974.

3. T.F. Stratton, et al., "Electron-Beam-Controlled CO_2 Laser Amplifiers," IEEE J. Quantum Electron. QE-9, No. 1, 157-163 (1973).

4. T.F. Deutsch and R.I. Rudko, "Spatial and Temporal Dependence of the Gain of a Transversely Excited Pulsed CO_2 Laser," Appl. Phys. Lett. 20, No. 11, 423-425 (1972).